

**LAND COVER CHANGE ASSESSMENT IN THE
BELEK FORESTLAND WITH MULTIDATE
SATELLITE IMAGERY USING CHANGE VECTOR
ANALYSIS TECHNIQUE**

**M.Sc.. Thesis by
Ayda F. AKKARTAL**

Department : Advance Technologies

Programme: Satellite Communication and
Remote Sensing

SEPTEMBER 2008

**LAND COVER CHANGE ASSESSMENT IN THE
BELEK FORESTLAND WITH MULTIDATE
SATELLITE IMAGERY USING CHANGE VECTOR
ANALYSIS TECHNIQUE**

**M.Sc.. Thesis by
Ayda F. AKKARTAL
(705041002)**

Date of submission : 20 May 2008

Date of defence examination: 12 September 2008

Supervisor (Chairman): Prof. Dr. Filiz SUNAR

Members of the Examining Committee Assoc. Prof.Dr. Çiğdem GÖKSEL (İTÜ)

Assoc. Prof.Dr. Berk ÜSTÜNDAĞ (İTÜ)

SEPTEMBER 2008

PREFACE

Environment is the combination of some key components such as the complete ecological units that function as natural systems without massive human intervention, including all vegetation, animals, microorganisms, rocks, atmosphere and natural phenomena that occur within their boundaries. Nature's resources must only be used at a rate at which they can be replenished naturally in order to be sustainable for the posterity of humankind on earth. There is now clear scientific evidence, that humanity is living in an unsustainable way, by consuming the Earth's limited natural resources more rapidly than they are being replaced by nature. Today, newly developed technologies such as remote sensing help us to keep human use of natural resources within the sustainable development aspect of the Earth's finite resource limits is now an issue of utmost importance to the present and future of humanity.

This thesis gave the opportunity to work and manifest an outcome on behalf of the protection and inspection of an environmental phenomenon, deforestation. Within all the possible topics, this one was a way out for me and took my interest during a brainstorming with my advisor and also director Prof. Dr. Filiz Sunar.

It gives me great a pleasure to acknowledge and thank all those people who have kindly given to me of their time, energy and support.

I thank most sincerely to Prof. Dr. Filiz Sunar for making this thesis possible and supporting me both academically and morally in all phases of this thesis.

I am grateful to all of my colleagues for their support and understanding, especially to Alper Akoguz for his valuable assistance in the programming phase.

I would also like to thank to my family for their endless support and patience.

I would like to thank to SPOT Image Inc. and SPOT Image team for all their contributions and support for providing and processing of the two SPOT-5 satellite images used in this thesis.

SEPTEMBER 2008

Ayda F. Akkartal

TABLE OF CONTENT

PREFACE.....	ii
ABBREVIATIONS.....	v
TABLE LIST	vii
FIGURE LIST	viii
SYMBOL LIST	x
ÖZET.....	xi
SUMMARY	xii
1 INTRODUCTION	1
2 FUNDAMENTALS OF REMOTE SENSING.....	8
2.1 Basic components of real remote sensing	9
2.2 Electromagnetic radiance	10
2.3 Electromagnetic waves.....	10
2.4 Electromagnetic spectrum	11
2.5 Energy Interactions with the Earth's Atmosphere	13
2.5.1 Absorption.....	13
2.5.2 Scattering.....	15
2.6 Interactions with the Earth Surface Materials	16
2.6.1 Specular reflectance	17
2.6.2 Diffuse reflectance	17
2.6.3 Albedo	18
2.6.4 Spectral Signatures.....	18
2.7 Spectral Reflectances of Earth Features	19
2.7.1 Spectral reflectance of vegetation	20
2.7.2 Spectral reflectance of soil	22
2.7.3 Spectral reflectance of water	22
3 REMOTE SENSING SATELLITES	23
3.1 Remote Sensing Satellites for Vegetation Studies	24
3.2 LANDSAT	27
3.2.1 LANDSAT System	28
3.2.2 Sensors	28
3.2.3 Vegetation and LANDSAT.....	30
3.3 SPOT	31
3.3.1 SPOT System	31
3.3.2 Sensors	32
3.3.3 Vegetation and SPOT.....	35
3.4 NOAA/AVHRR	36
3.4.1 AVHRR System	36
3.4.2 Sensors	37
3.4.3 Vegetation and NOAA/AVHRR.....	37
3.5 MODIS	38
3.5.1 Terra MODIS System	39
3.5.2 Aqua MODIS System	39
3.5.3 Vegetation and MODIS.....	40

4	DIGITAL IMAGE PROCESSING	43
4.1	Image Resolution.....	43
4.1.1	Spatial Resolution	44
4.1.2	Spectral Resolution	45
4.1.3	Radiometric Resolution.....	46
4.1.4	Temporal Resolution.....	47
4.2	Preprocessing.....	48
4.2.1	Geometric Corrections	48
4.2.2	Radiometric Corrections	49
4.3	Image Ratio	49
4.3.1	Normalized Difference Vegetation Index (NDVI)	50
4.3.2	Difference Vegetation Index (DVI)	51
4.3.3	Soil Brightness Index (SBI)	51
4.4	Change Vector Analysis (CVA).....	51
4.4.1	Preprocessing requirements of CVA.....	55
5	APPLICATION	57
5.1	Study Area and Data Used	57
5.2	Methodology	59
5.3	Geometric and radiometric correction.....	60
5.4	NDVI differencing	62
5.5	Change vector analysis	64
6	RESULTS	69
	REFERENCES.....	62
	ANNEX-1	76
	ANNEX-2	78
	ANNEX-3	80
	ANNEX-4	81

ABBREVIATIONS

AVHRR	: Advanced Very High Resolution Radiometer
CCD	: Charge Coupled Device
CNES	: Centre National d'Etude Spatiales
CVA	: Change Vector Analysis
DN	: Digital Number
DVI	: Difference Vegetation Index
ESA	: European Space Agency
ETM	: Enhanced Thematic Mapper
EVI	: Enhanced Vegetation Index
FAO	: The Food and Agriculture Organization of the UN
GAC	: Global Area Coverage
GCP	: Ground Control Points
GIS	: Geographical Information System
GPS	: Global Positioning System
HRG	: High Resolution Geometric
HRPT	: High Resolution Picture Transmission
HRS	: High Resolution Stereoscopic
HRV	: High Resolution Visible
HRVIR	: High Resolution Visible IR
IFOV	: Instantaneous Field of View
IR	: Infrared
ITU-CSCRS	: Istanbul Technical University – Center of Satellite Communication and Remote Sensing
LAI	: Leaf Area Index
LAC	: Local Area Coverage
LWIR	: Long Wave Infrared
NIR	: Near Infrared
MODIS	: Moderate-resolution Imaging Spectroradiometer
MS	: Multispectral Image
MSS	: Multi-Spectral Scanner
MWR	: Microwave Radiometer
NASA	: National Aeronautics and Space Administration
NDVI	: Normalized Difference Vegetation Index
NOAA	: National Oceanic and Atmospheric Administration
PAN	: Panchromatic image
RADAR	: Radio Detecting and Ranging
POES	: Polar Orbiting Environmental satellites
PVI	: Perpendicular Vegetation Index
RMS	: Root Mean Square
RVI	: Simple Ratio Vegetation Index
SAR	: Synthetic aperture radar
SBI	: Soil Brightness Index

SPOT	: Systeme Probatoire pour l'Observation de la Terre
SWIR	: Short Wave Infrared
TIR	: Thermal Infrared
TM	: Thematic Mapper
TVI	: Transformed Vegetation Index
USGS	: U.S. Geological Survey
UV	: Ultraviolet
VNIR	: Visible and Near Infrared

TABLE LIST

Table 3.1	: Main features of image products from different sensors	26
Table 3.2	: Landsat MSS sensor characteristics.....	29
Table 3.3	: TM bands	29
Table 3.4	: Landsat TM, ETM+ sensor characteristics	30
Table 3.5	: Spot HRV and HRVIR instrument characteristics	32
Table 3.6	: HRV spectral bands	34
Table 3.7	: HRVIR spectral bands	34
Table 3.8	: HRG spectral bands	34
Table 3.9	: AVHRR sensor characteristics	37
Table 3.10	: MODIS Band 1-19 sensor characteristics.....	41
Table 3.11	: MODIS Band 20-36 sensor characteristics.....	42
Table 4.1	: Factors in choice of the CVA Approach.....	52
Table 5.1	: Spectral and spatial resolutions of the data used	59
Table 5.2	: Min. and max. values of the bands used	62
Table 5.3	: The appearance of the NDVI difference outputs	64

FIGURE LIST

Figure 1.1	: The world's forests	1
Figure 1.2	: Areas affected by deforestation from 1970 to 1990	2
Figure 1.3	: Deforestation rates between 1990 and 2000.....	2
Figure 1.4	: Worldwide distribution of tropical and temperate forests	3
Figure 1.5	: Land usage chart of Turkey	3
Figure 1.6	: Forest cover map of Turkey in 2000	4
Figure 1.7	: The effects of deforestation	5
Figure 1.8	: Land use/cover changes detected by satellite images.....	6
Figure 2.1	: (a) Passive and (b) active remote sensing.....	8
Figure 2.2	: Basic remote sensing components.....	9
Figure 2.3	: Characteristic of an electromagnetic wave.....	10
Figure 2.4	: The electromagnetic spectrum.....	11
Figure 2.5	: Wavelength in nanometres	12
Figure 2.6	: Wavelength versus energy and transmission.....	15
Figure 2.7	: Atmospheric transmission windows	15
Figure 2.8	: Atmospheric scattering	15
Figure 2.9	: Reflectance types	17
Figure 2.10	: Albedo values of different surface materials.....	18
Figure 2.11	: Spectral reflectance curves for common cover types	19
Figure 2.12	: Spectral reflectance curve of vegetation.....	20
Figure 2.13	: Spectral reflectance of different tree species	21
Figure 3.1	: Main Earth feature's spectral reflectances.....	25
Figure 3.2	: (a) Landsat-7 satellite, (b) An example of Landsat-7 scene	28
Figure 3.3	: (a) SPOT 5 satellite, (b) An example of SPOT 5 scene	31
Figure 3.4	: SPOT 5 Supermode processess	35
Figure 3.5	: (a) NOAA satellite, (b) An example of NOAA-17 scene	36
Figure 3.6	: (a) Aqua satellite, (b) Terra satellite, (c) An example of Terra.....	39
Figure 4.1	: Digital image representation.....	43
Figure 4.2	: Toulouse, viewed at different resolutions	44
Figure 4.3	: Differences in spatial resolution among some well known sensors ...	45
Figure 4.4	: The comparison between the colour film and the black/white film ...	46
Figure 4.5	: Spot Panchromatic images with different radiometric resolutions.....	47
Figure 4.6	: Flow diagram of CVA based change detection	54
Figure 4.7	: Representation of change vector in 2-band	55
Figure 5.1	: The map of the study area	57
Figure 5.2	: Tourism regions of Antalya.....	58
Figure 5.3	: Aerial photographs of the Belek Forests	58
Figure 5.4	: Methodology used in this study.....	60
Figure 5.5	: The distribution of the GCPs in the second image	60
Figure 5.6	: The list of the GCPs selected and the errors (X, Y and RMS).....	61
Figure 5.7	: Registered and masked images of the study area	62
Figure 5.8	: NDVI differencing image	63
Figure 5.9	: An example showing high NDVI difference.....	63

Figure 5.10 : Soil Brightness Index images	64
Figure 5.11 : Difference Vegetation Index images	65
Figure 5.12 : The process for detecting.....	66
Figure 5.13 : Transferring bands to Matlab Environment	66
Figure 5.14 : The graph indicating the total number of pixel distribution.....	67
Figure 5.15 : Deforestation in the study area with the threshold value of 26 DN ...	68
Figure 5.16 : Deforestation in the study area with the threshold value of 80 DN ...	68

SYMBOL LIST

λ	: Wavelength
ν	: Frequency
h	: Planck constant (6.6260×10^{-34} jul/sn)
c	: Speed of light 3×10^8 m/s
E	: Energy
σ^2	: Variance
$E_R(\lambda)$: Reflected energy
$E_A(\lambda)$: Absorbed energy
$E_T(\lambda)$: Transmitted energy

ÇOK ZAMANLI UYDU GÖRÜNTÜLERİ İLE BELEK ORMANLIK ALANLARINDAKİ ARAZİ ÖRTÜSÜ DEĞİŞİMİNİN VEKTÖR DEĞİŞİM ANALİZİ YÖNTEMİ İLE DEĞERLENDİRİLMESİ

ÖZET

Yeryüzü örtüsündeki ve kullanımındaki değişikliklerin çoklu spektral uydu görüntüleri ile saptanması ve izlenmesi uzaktan algılamada önemli bir yere sahiptir. Gelişen teknikler, yeryüzü örtüsü ve kullanımındaki değişikliklerin incelenmesine çok uygun olup yüksek doğrulukta sonuçlara ulaşılmasını sağlamaktadır. Spektral kategorileme (sınıflandırma) ve değişim saptama amaçlı radyometrik değişim genel başlıkları altında farklı teknikler formüle edilmiş, uygulanmış ve bir çok çevresel uygulamada değerlendirilmiştir. Çok zamanlı ve çoklu spektral veriler ile değişim analizi yapmaya ve işlemeye olanak veren vektör değişim analizi (CVA), yeryüzü örtüsünde meydana gelen değişimlerin belirlenmesi ve karakterize edilmesinde etkili bir yaklaşımdır. Bu bağlamda, çalışmanın ana hedefi; Antalya Belek orman alanlarındaki arazi örtüsü ve kullanımı değişiminin radyometrik bir teknik olan vektör değişim analizi yöntemi baz alınarak saptanmasıdır.

Bu çalışmada, band farkı ve CVA gibi radyometrik değişim analiz teknikleri, Belek ormanlık alanlarında ağaç kesiminden dolayı meydana gelen ormansızlaşmanın izlenmesinde kullanılmıştır. Genel olarak, band farkı analizi genel değişim ve bunun belirlenebilirliği hakkında bilgi verirken, CVA bitki örtüsünde meydana gelen değişimin yönü ve yoğunluğu hakkında niteliksel bilgi vermektedir. CVA analizinde fark bitki indeksinin (DVI) ve toprak parlaklık indeksinin (SBI) kullanımı ile bantların boyutluluğu azatılarak aynı zamanda bölgenin bitkisel özelliklerinin ön plana çıkarılması sağlanmaktadır. CVA yaklaşımının çok zamanlı veri üzerinde daha hassas ve mevsimsel küçük değişimler ile bitki fenolojisi hakkında diğer klasik yaklaşımlara göre daha fazla bilgi sağladığı gözlenmiştir.

Anahtar Kelimeler: Uzaktan algılama, Vektör değişim analizi, Ormansızlaşma, Çok zamanlı ve çoklu spektral görüntü

Bilim Dalı Sayısal Kodu: 616.02.04

LAND COVER CHANGE ASSESSMENT IN THE BELEK FORESTLAND WITH MULTIDATE SATELLITE IMAGERY USING CHANGE VECTOR ANALYSIS TECHNIQUE

SUMMARY

The detection and monitoring of land use / land cover change using satellite multispectral imagery has been a topic of interest in remote sensing. Progressive techniques are very adequate to analyze the changes in land cover/use with a high accuracy. Different techniques, mostly grouped into two general classes based on spectral categorization (classification) and radiometric change for accomplishing change detection, have been formulated, applied and evaluated in many environmental applications. Change vector analysis is an effective approach for detecting and characterizing land cover change that processes and analyses change in all multi-spectral and multi-temporal data. In this context, the main objective of this paper is to authenticate the land cover change based on a radiometric technique, Change Vector Analysis (CVA) for the Belek forestland in Antalya.

As shown in this study, radiometric change techniques such as band differencing and CVA were used to detect the deforestation due to woodcutting in Belek forests. In general band differencing gives information about the general change and its detectability whereas CVA offers qualitative information concerning the direction and the intensity of the change occurred in vegetation. The conversion of the bands to DVI and SBI reduced the dimensionality of the bands and at the same time highlighted vegetative properties of the landscape. It was seen that, CVA approach of multitemporal data is more sensitive to, and provides more information on, subtle changes regarding to seasonality and vegetation phenology than other classic approaches.

Keywords: Remote sensing, Change vector analysis, Deforestation, Land cover, Multitemporal and mutispectral imagery

Bilim Dalı Sayısal Kodu: 616.02.04

1 INTRODUCTION

The growth in the population of Earth and the needs of human beings causes unintentional deformation of natural resources more and more. The perishing of natural resources affects the wild life, ecological balance, food chain and finally the life of posterity. As a result, planners and resource managers need reliable mechanism to assess these consequences by detecting, monitoring and analyzing land use changes quickly and effectively.

The total forest area is about 4 billion hectares (3 952 million hectares or about 40 million km²) or 30.3 percent of total land area of the world (Figure 1.1). Forests ensure environmental functions such as biodiversity, water and soil conservation, water supply and climate regulation. They provide habitats to about two-thirds of all species on earth (FOA, 2008). According to the World Resources Institute, more than 80 percent of the Earth's natural forests already have been destroyed.

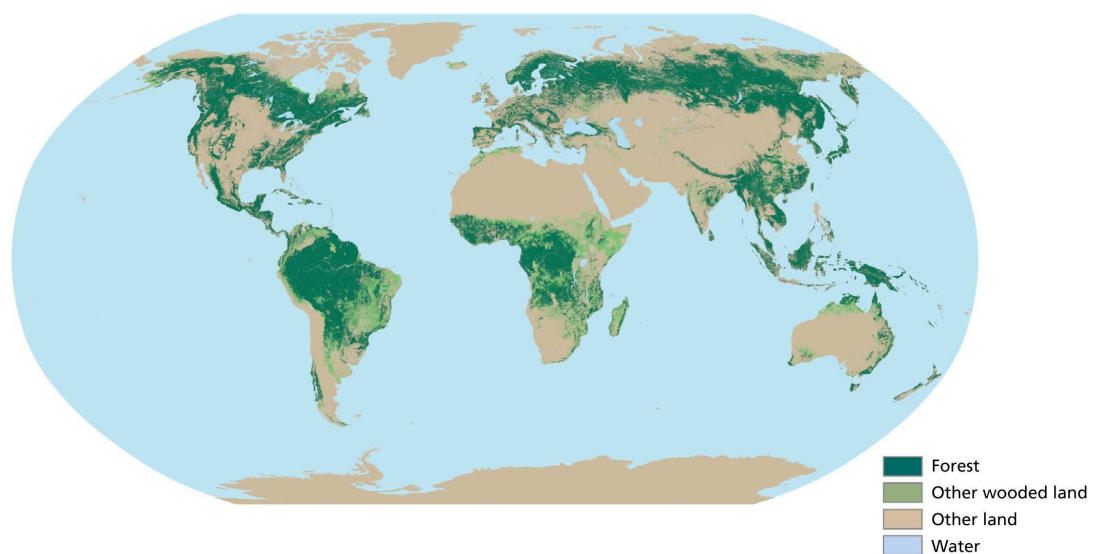


Figure 1.1 The world's forests (FAO, 2008)

The Food and Agriculture Organization of the UN (FAO) uses the definition of deforestation as the removal of forest cover to an extent that allows for alternative land use. Each year about 13 million hectares of the world's forests are lost due to deforestation, but the rate of net forest loss is slowing down due to new planting and natural expansion of existing forests (FOA, 2008) (Figure 1.2). For example, from 1990 to 2000 (Figure 1.3), the net forest loss was 8.9 million hectares per year on the other hand from 2000 to 2005, the net forest loss was 7.3 million hectares per year (FOA, 2008).



Figure 1.2 Areas affected by deforestation from 1970 to 1990 (Rekacewicz; 2002)

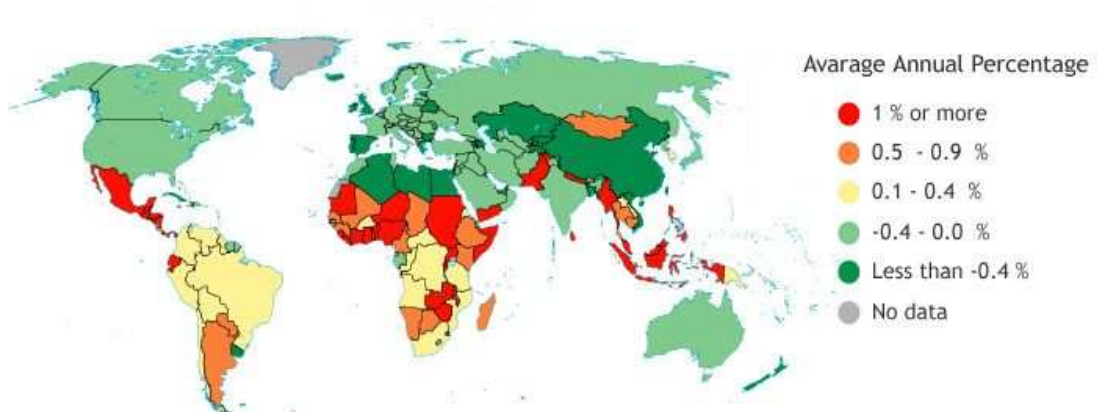


Figure 1.3 Deforestation rates between 1990 and 2000

Based on its location between Asia, Europe and Africa, Turkey has various flora and fauna, comprised of elements of all these continents. As well as being a repository of plants and animals from many different countries, forests of Turkey is also a shelter

to several species of plants exists nowhere else on the planet. Of the 9,000 plant species in Turkey, 3,000 species are endemic to Turkey (Nigros, 2003). Moreover, the temperate broadleaf forests; where the biodiversity is concentrated much closer to the forest floor, are present among the Mediterranean coast (Figure 1.4). These forests should be considered as one of the Turkey's preservation areas. As in any rapidly developing country, Turkey's enormous population growth destroys habitats and displaces many species of animals.

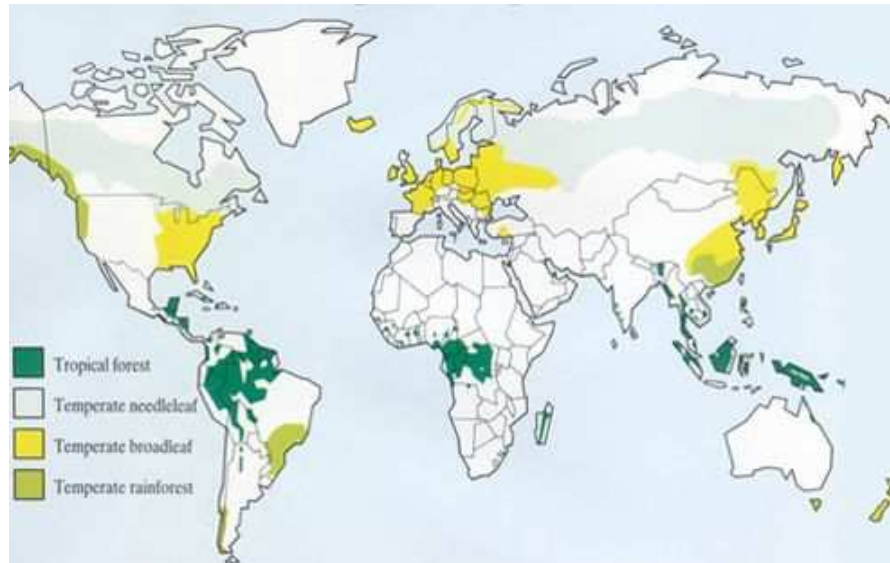


Figure 1.4 Worldwide distribution of tropical and temperate forests
(UNESCO, 2008)

All over the world, the rate of forest coverage have to be at least 30 percent for each country, to be considered as sufficient, while this value is 27.2 for Turkey (Figure 1.5). This is close to the world aggregate forest rate; however 49 percent of Turkey's forests are non-productive thus is classified as insufficient (Figure 1.6) (Ekmen & Topçu, 2008).

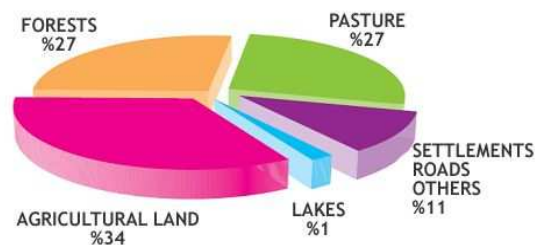


Figure 1.5 Land usage chart of Turkey

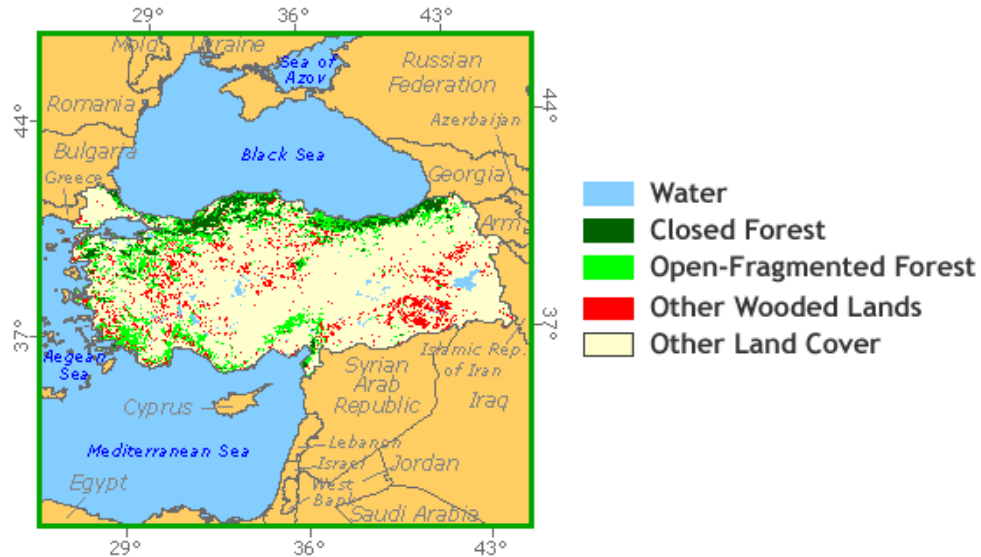


Figure 1.6 Forest cover map of Turkey in 2000 (FOA, 2008)

In 2005, the forest cover of Turkey was as follows (Butler, 2006);

Total land area	: 76,963,000 ha
Total forest area	: 10,175,000 ha
Percent forest cover	: 13.22%
Primary forest cover	: 975,000 ha
Primary forest, % total forest	: 9.58%
Primary forest, % total land	: 1.27%
Other wooded land	: 10,689,000 ha

In general, the direct causes of deforestation can be listed as the population growth, agriculture and cattle-raising, dams and mega projects, forest fires, logging, mangroves and shrimp farming, mining, oil and gas, plantations. Once initiated, it is almost impossible to stop, and it can not be reversed within a human lifetime.

The role of population in deforestation varies considerably from one setting to another depending on the local patterns of human occupancy and economic activity. Increasing population rises the demands for land and wood, eventually exceeding the carrying capacity of forests that are expected to supply wood fuels, food, and environmental protection for inhabitants.

Forest fires can be started deliberately or naturally and are becoming more common as temperatures rise. Large areas tend to go up in flames rapidly threatening not only the forest itself but also crops and settlements nearby.

Logging operations, which provide the world's wood and paper products, also involves cutting of countless trees each year legally and mostly illegally.

It is said by Dr. Aykut Kence, of Middle East Technical University's Department of Biology that "There is an attempt to change the constitution of Turkey to allow for the sale of lands that were once classified as forests because they have lost the properties that a forest must have" (Nigros, 2003). This intention of the government encourages people to cause the forest areas to lose their properties as a forest. Moreover some valuable areas were deforested by declaring them as touristic zones.

Whatever the cause is, deforestation presents multiple social and environmental problems. Some effects of deforestation are erosion, landslides, disruption of the water cycle, flooding, loss of biodiversity, drought, destruction of floral and faunal habitat and last but not least the climate change resulting in global warming (Figure 1.7).

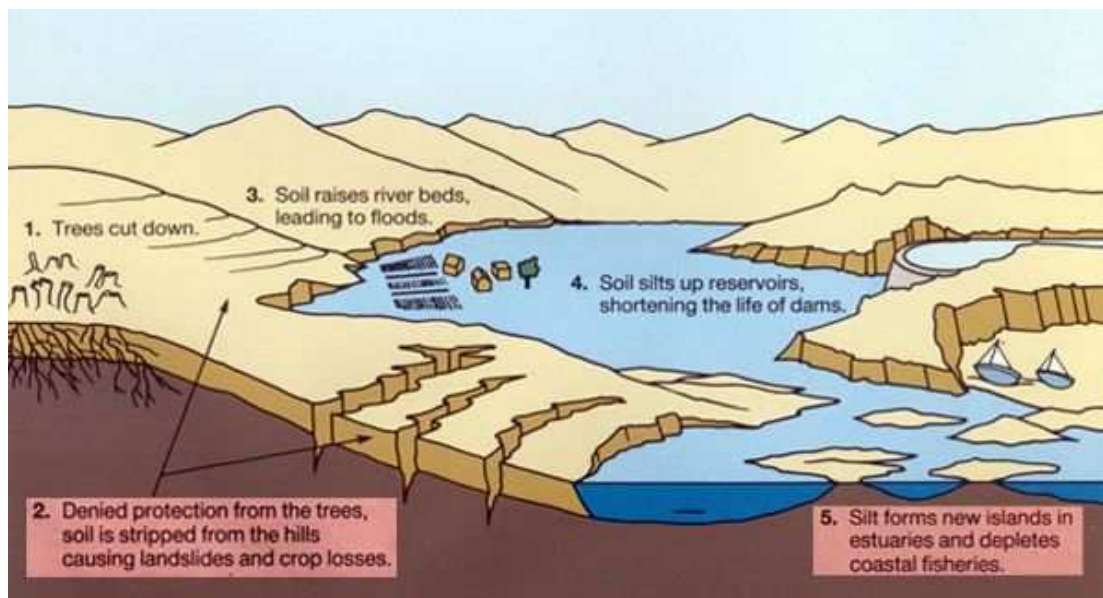


Figure 1.7 The effects of deforestation (UNESCO, 2008)

As the forests help to retain moisture in the air, its absence causes an abrupt change in temperature in the nearby areas. Higher amount of harmful rays penetrating the atmosphere increases the world's climates become warmer, contributing to the global warming. On the other hand underground water table is the common source of

natural drinking water by people living around forests. Forests hold most of the rainfall to the soil through their roots and help the water table to replenish regularly. Moreover, it is estimated that there are millions of plant and exist animal species that have been wiped out due to being deprived of home (Fiset, 2008). The social impact of deforestation strongly shows itself threatening the living conditions of indigenous people who consider forests as their primary habitats.

The monitoring and detection of land use/cover change using satellite multispectral imagery has been an important topic in remote sensing (Figure 1.8). A number of techniques for realizing the detection of land cover dynamics using remotely sensed imagery have been formulated, tested and assessed with the results varying with respect to the change scenario under investigation, the information required and the imagery applied (Siwe & Koch, 2008). Most of these techniques can be grouped into two general classes: (1) those based on spectral categorization (classification) of the input data; and (2) those based on radiometric change between acquisition dates (Johnson & Kasischke, 1998).



Figure 1.8 Land use/cover changes detected by satellite images of Iguazú National Park, located in Argentina near Brazil and Paraguay (UNEP, 2008)

Monitoring change in vegetation between two time periods can assess the health and vigor of forest and plant species, assess vegetation growth and regrowth following a cataclysmic event, or quantify forest loss caused by deforestation and timber harvesting (Lawrence & Ripple, 1999). These changes can be classified effectively using the change vector analysis (CVA) (Lambin & Strahler, 1994; Johnson & Kasischke, 1998; Allen & Kupfer, 2000; Lorena et al, 2002; Lunetta et al, 2004). CVA is a radiometric technique that examines corresponding pixels of two maps by comparing two bands of each map to produce images of change direction and change magnitude (Kuzera et al, 2005).

Antalya\Belek is unique in its climate and geography, and also exceptionally rich in its historical, natural and biological resources. Belek forestlands, the worlds second great stone pine area, was planted in 1960's. It was the region's and one of Turkey's most important ecosystem that sheltered 27 species and 1 sub species of endemic plants, 109 birds that are under danger with average of 600 – 700 thousand trees spread over 2300 hectares area (Cyprus Observer, 2007; Kaiser, 2008). Besides, Belek region is the second largest known nesting area for sea turtles after the Zakynthos Island of Greece (Canbolat, 2000).

Owing to the ecological diversity in the region, and the crucial role played by the forests in inhibiting dune movement on the coastline, the government has taken preventive measures to protect the forested land in and around Belek by granting it the status of a conservation forest. The Serik Forest Enterprise, a public organization, is in charge of the management of this forest. In the establishment of conservation forests, the main consideration is nature protection for the sake of soil and water resources and the plant cover, with human uses such as recreation and tourism coming second in importance (Kuvan, 2005).

Today, the Belek forests are being destined to golf areas and tourism resorts. A considerable part of the region was sentenced as a "Tourism Development Area" and a number of tourism establishments have been constructed. Now, the region has 45 four or five-stars hotels and first-class holiday villages and six golf courses (Cyprus Observer, 2007). The most important impact of the allocation of forest lands to tourism facilities is undoubtedly the reduction in forest area and number of trees.

In this thesis, changes in Belek forestland were analyzed using multitemporal satellite data. The SPOT -5 multispectral satellite images of the area covering the forest and destined areas in Belek Antalya were acquired by SPOT Image on the 27th of October, 2005 and 23rd of May, 2007, respectively and analyzed by ITU-CSCRS (Istanbul Technical University – Center of Satellite Communication and Remote Sensing). After the preprocessing step, CVA was applied to the Greenness and Brightness variables that were calculated from three multispectral bands (having 5 m spatial resolution) of SPOT -5 images. The output was the change image indicating the change vector direction and the multispectral change magnitude that gave information about the amount of the change in the forested area.

2 FUNDAMENTALS OF REMOTE SENSING

Remote sensing is the technology of gathering information of the earth surface and atmosphere by airborne or space borne satellites without any physical interaction. The materials of earth and atmosphere are not detected directly with this technology. Their nature is inferred from the properties of the radiance measurements. (Mather, 1987)

There are two different types of sensors. They are active and passive sensors (Figure 2.1). A passive sensor uses naturally reflected or emitted energy of the imaged surface and with these kinds of sensors images of visible, near-infrared and thermal infrared energy can be obtained. Active remote sensing sensors provide their own illumination and measure the energy that comes back. This technology is used in lidar and radar.

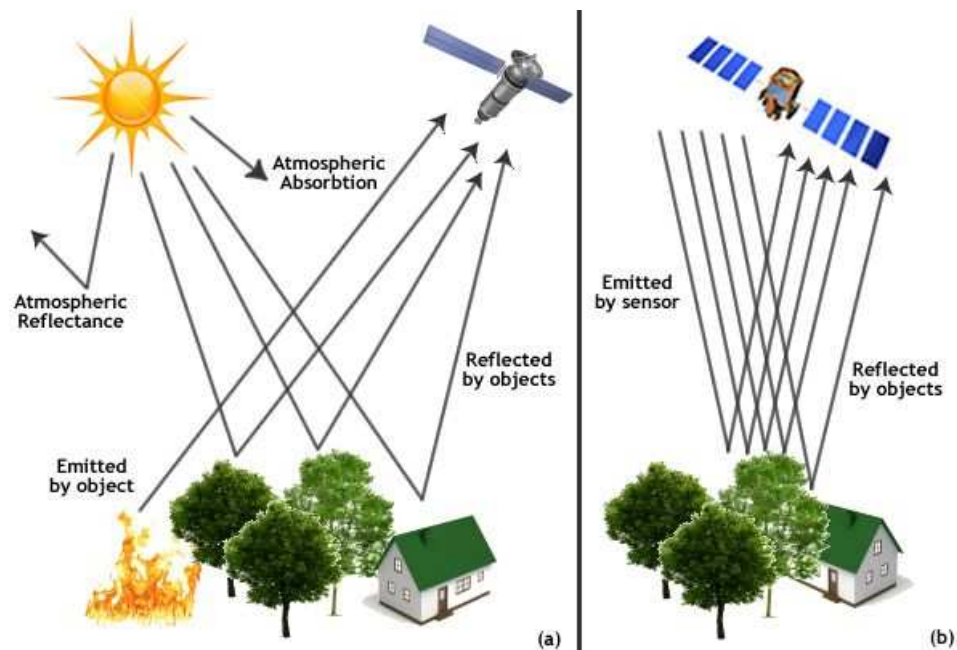


Figure 2.1 (a) Passive and (b) active remote sensing

2.1 Basic components of real remote sensing

1. **An energy source:** The source provides energy over all wavelengths at a constant, known, high level of output, irrespective of time and place.
2. **The atmosphere:** Atmosphere modifies the energy from the source in any manner when the energy is on its way to earth or to satellite.
3. **Energy interactions at the earth surface:** These should generate reflected or emitted signals that not only selected due to wavelength but also invariant and unique to each and every earth surface feature type.
4. **The sensor:** The sensors are sensitive to wavelengths yielding spatially detailed data on absolute brightness as a function of wavelength. Also it has to be simple, reliable, be accurate and economical to operate.
5. **A data handling system:** The radiance versus wavelength response over a terrain element was generated. It would be processed into an interpretable format and recognized as unique to the particular terrain element from which it came. The process should be real time due to the nature of the energy.
6. **Multiple data users:** These people should have knowledge in remote sensing data acquisition and analyses technique (Figure 2.2). (Lillesand ,1987)

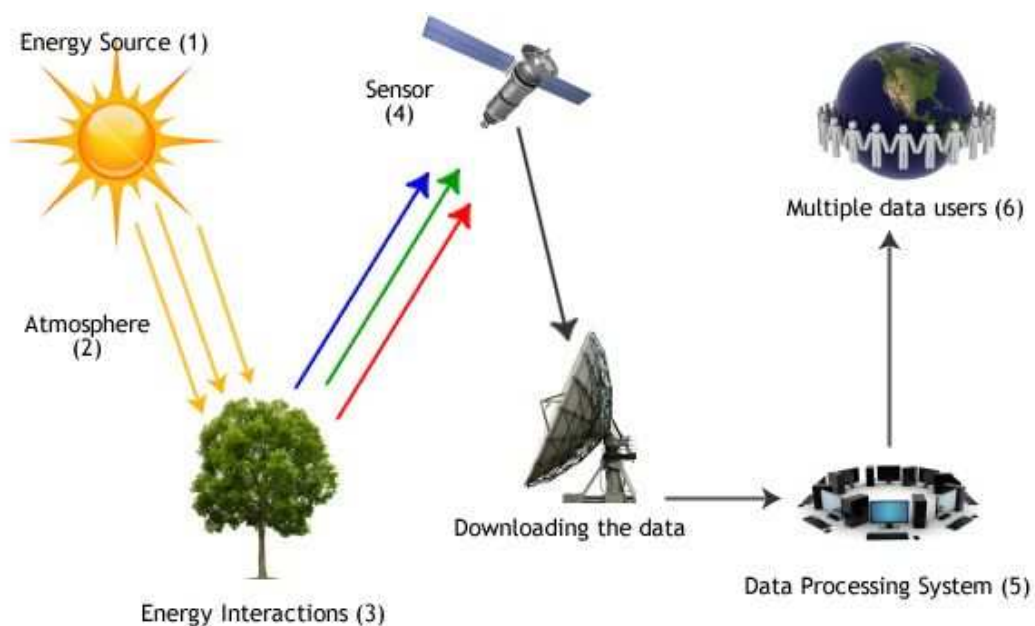


Figure 2.2 Basic remote sensing components

2.2 Electromagnetic radiance

Electromagnetic radiance is used to carry information to the sensors. Electromagnetic radiation with individual temporal and spatial properties is used in remote sensing to transmit information about an object; also time and space are the terms of specific characteristics of electromagnetic radiation. The wave-like characteristic of electromagnetic radiation gives the ability of distinguishing between different manifestations of radiation such as microwave or infrared radiation. This also helps to understand the interactions between electromagnetic energy and the Earth's atmosphere. This way of thinking rises the idea of light existing of a stream of particles or photons is most easily used. Electromagnetic radiation is both a wave and a stream of particles can be said depending to the quantum mechanics. (Mather, 1987)

2.3 Electromagnetic waves

Electromagnetic waves are energy transported through space in the form of periodic interfere with electrical and magnetic fields. These waves travel through the space in the speed of light, which is 2.99792458×10^8 m/s in the form of sinusoidal waves. Electromagnetic waves are characterized by a frequency and a wavelength (Figure 2.3). The micron is the basic unit for measuring the wavelength of electromagnetic waves (CRISP, 2001). The frequency and the wavelength of electromagnetic waves depend on the source.

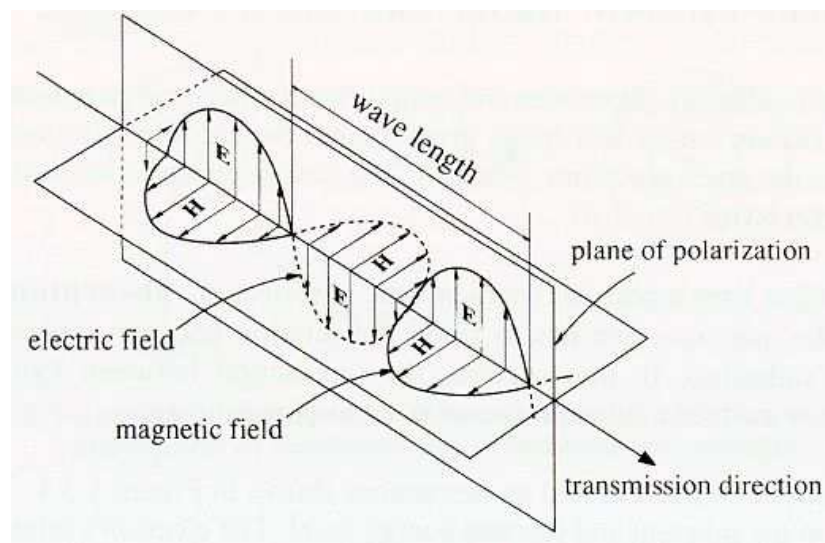


Figure 2.3 Characteristic of an electromagnetic wave

2.4 Electromagnetic spectrum

The electromagnetic spectrum is a continuum of all kinds of electromagnetic waves in order to their frequency and wavelength. The spectrum of waves is divided into sections based on wavelength (Figure 2.4). The shortest waves are gamma rays, which have wavelengths of 10^{-6} microns or less. The longest waves are radio waves, which have wavelengths of many kilometers. (Schneider, 2007)

Wavelength units: 1 mm = 1000 μm ; 1 μm = 1000 nm.

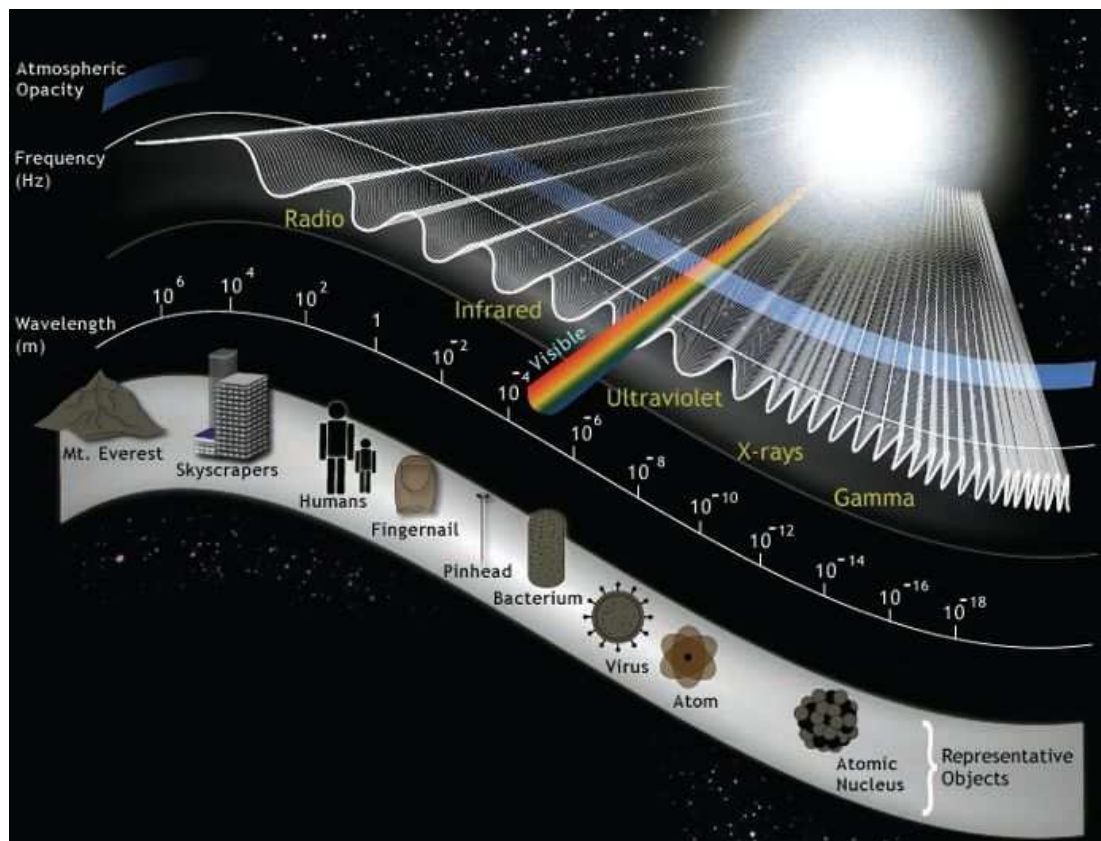


Figure 2.4 The electromagnetic spectrum

– Radio waves

Radio waves have 10 cm to 10km wavelength. These wavelengths are used in remote sensing but not in detecting Earth surface phenomena. Commands that are sending to the satellite make use of radio wavelengths. Image data are transmitted to ground receiving stations using these wavelengths and data are recorded by high-speed tape recorders while the satellite is in direct line of sight with the ground receiving station. (Mather, 1987)

– Microwaves

The region of the spectrum that is composed of electromagnetic radiation with wavelengths between 1 mm and 300 cm is called microwave band. These levels are too low for high-resolution image generation. In order to this most microwave sensors can both generate and detect their own source of radiation. This kind of active microwave imaging systems is called as radar. (Mather, 1987)

– Infrared

Infrared band extends from 0.7 μm to 1mm, which is not very uniform. Short wavelength or near infrared behaves like visible light and can be detected by special photographic films. Infrared radiation with a wavelength of up to 3.0 μm is primarily of solar origin and, like visible light, is reflected by the surface of the Earth. Beyond a wavelength of 3.0 μm infrared radiation emitted by the Earth's surface can be detected in the form of heat. In order to sensing in the form of heat these wavelengths are called thermal infrared. (Mather, 1987)

– Visible light

Visible light is so called because the eye can detect it, where as other form of electromagnetic spectrum radiation, in general, cannot. (Mather, 1987) This narrow band of electromagnetic radiation extends from about 400nm (violet) to about 700nm (red), which corresponds to the wavelengths near the maximum of the Sun's radiation curve. (Figure 2.5) In order to this visible light primarily acts to set elevate electrons to higher energy levels. (CRISP, 2001)

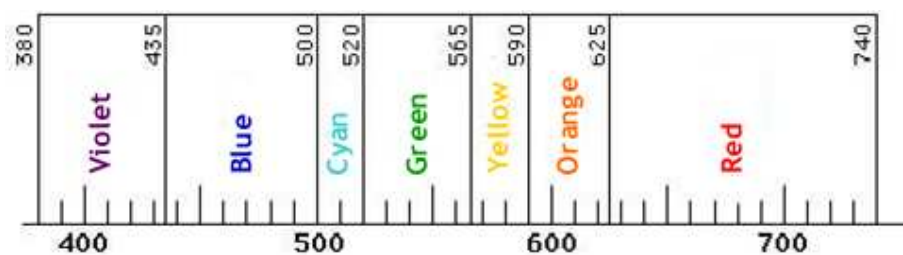


Figure 2.5 Wavelength in nanometres

– Ultraviolet

It is absorbed very strongly by most solid substances, and even absorbed appreciably by air. The shorter wavelengths reach the ionisation energy for many molecules, so the far ultraviolet has some of the dangers attendant to other ionising radiation. The

sun is a strong source of ultraviolet radiation, but atmospheric absorption eliminates most of the shorter wavelengths. An ultraviolet wavelength extends from 400nm to 10nm. (Hyperphysics, 2005)

– X-rays

X-ray was the name given to the highly penetrating rays, which emanated when high-energy electrons struck a metal target. They are high frequency electromagnetic rays, which are produced when the electrons are suddenly decelerated. X-rays are also produced when electrons make transitions between lower atomic energy levels in heavy elements. They extend from 10nm to downward. (Hyperphysics, 2005)

– Gamma Rays

The term gamma ray is used to denote electromagnetic radiation from the nucleus as a part of a radioactive process. The energy of nuclear radiation is extremely high because such radiation is born in the intense conflict between the nuclear strong force and the electromagnetic force, the two strongest basic forces. (Hyperphysics, 2005)

2.5 Energy Interactions with the Earth's Atmosphere

When electromagnetic radiation travels through the atmosphere, it may be absorbed or scattered by the constituent particles of the atmosphere. Molecular absorption converts the radiation energy into excitation energy of the molecules. Scattering redistributes the energy of the incident beam to all directions. The overall effect is the removal of energy from the incident radiation. They limit the usefulness of some portions of the electromagnetic spectrum for the remote sensing purposes. The reduction in light through the atmosphere by absorption and scattering is called attenuation or extinction. (Mather, 1987)

2.5.1 Absorption

Atmospheric absorption results in the effective loss of energy atmospheric constituents. The most efficient absorbers of solar radiation are water vapour, carbon dioxide, and ozone.

Atmospheric absorption affects mainly the visible and infrared bands. Optical remote sensing depends on solar radiation as the source of illumination. Absorption reduces the solar radiance within the absorption bands of the atmospheric gases. The

reflected radiance is also attenuated after passing through the atmosphere. This attenuation is wavelength dependent. Hence, atmospheric absorption will alter the apparent spectral signature of the target being observed. (CRISP, 2001)

$$E = (hc) / \lambda \quad (2.1)$$

In the formulation;

h: Planck constant (6.6260×10^{-34} jul/sn),

c: 3×10^8 m/s,

λ : Wavelength,

E: Energy.

There is little absorption of the electromagnetic radiation in the visible part of the spectrum. The absorption in the infrared region is mainly due to rotational and vibrational transitions of the molecules. The main atmospheric constituents responsible for infrared absorption are water vapour and carbon dioxide molecules. Because these molecules have absorption bands centered at the wavelengths from near to long wave infrared. In the far infrared region, the atmosphere absorbs most of the radiation. On the other hand the atmosphere is transparent to the microwave radiation.

Each type of molecule has its own set of absorption bands in various parts of the electromagnetic spectrum (Figure 2.6). As a result, only the wavelength regions outside the main absorption bands of the atmospheric gases can be used for remote sensing. These regions are known as the Atmospheric Transmission Windows (Figure 2.7). The wavelength bands used in remote sensing systems are usually designed to fall within these windows to minimize the atmospheric absorption effects. These windows are found in the visible, near infrared, certain bands in thermal infrared and the microwave regions. (CRISP, 2001)

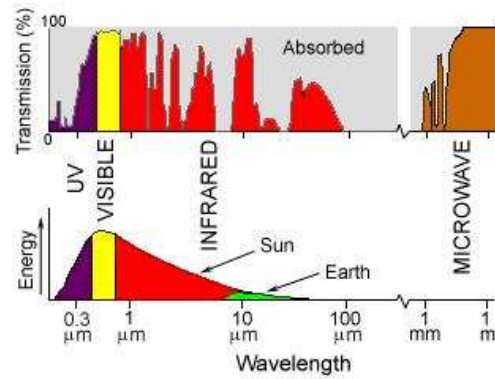


Figure 2.6 Wavelength versus energy and transmission % through the electromagnetic spectrum

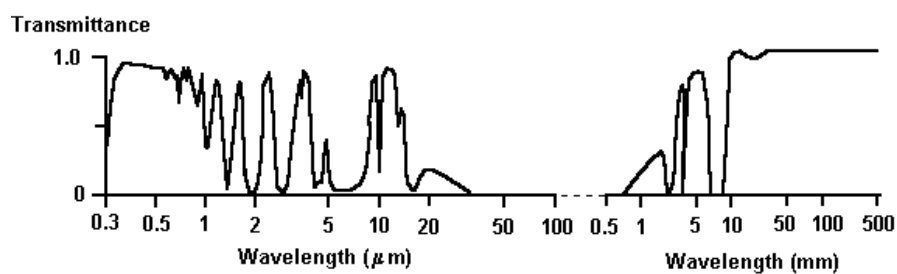


Figure 2.7 Atmospheric transmission windows

2.5.2 Scattering

Scattering of electromagnetic radiation is caused by the interaction of radiation with matter resulting in the reradiating of part of the energy to other directions not along the path of the incident radiation. Scattering effectively removes energy from the incident beam. Unlike absorption, this energy is not lost, but is redistributed to other directions. Both the gaseous and aerosol components of the atmosphere cause scattering in the atmosphere (CRISP, 2001). There are three different scattering types depending on the atmospheric particle diameter and the wavelength of the interacting radiation. These are called Rayleigh, Mie and Non-selective scattering (Figure 2.8).

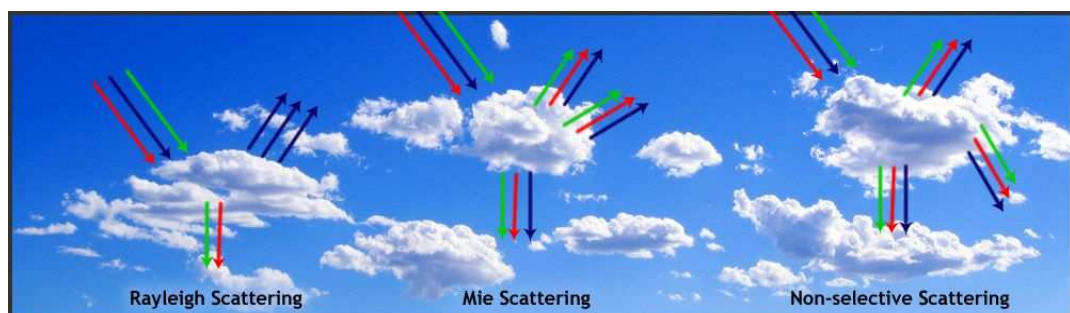


Figure 2.8 Atmospheric scattering

Atmospheric scattering is important only in the visible and near infrared regions. Scattering of radiation by the constituent gases and aerosols in the atmosphere causes degradation of the remotely sensed images. The solar radiation scattered by the atmosphere towards the sensor without first reaching the ground produces a hazy appearance of the image. This effect is particularly severe in the blue end of the visible spectrum due to the stronger Rayleigh scattering for shorter wavelength radiation. Also, the light from a target outside the field of view of the sensor may be scattered into the field of view of the sensor. This effect is known as the adjacency effect. Near to the boundary between two regions of different brightness, the adjacency effect results in an increase in the apparent brightness of the darker region while the apparent brightness of the brighter region is reduced. Scattering also produces blurring of the targets in remotely sensed images due to spreading of the reflected radiation by scattering, resulting in a reduced resolution image. (CRISP, 2001)

2.6 Interactions with the Earth Surface Materials

Three main energy interactions occur with a feature of interest when electromagnetic energy is incident on any given earth surface feature. These are reflected, absorbed and transmitted energy. (Agouris, 2005) On average, 51% of the in-coming solar radiation reaches the Earth's surface. Of this total, 4% is reflected back into the atmosphere and 47% is absorbed by the Earth's surface to be re-radiated later in the form of thermal infrared radiation Through the law of conservation of energy the incident energy equals the sum of the reflected energy, the absorbed energy and the transmitted energy, all of which are functions of wavelength.

$$E_I(\lambda) = E_R(\lambda) + E_A(\lambda) + E_T(\lambda)$$

$$\begin{aligned} 1 &= E_R(\lambda)/E_I + E_A(\lambda)/E_I + E_T(\lambda)/E_I \\ &= r(\lambda) + a(\lambda) + t(\lambda) \end{aligned} \tag{2.2}$$

Where $E_R(\lambda)$ is the reflected energy, $E_A(\lambda)$ is the absorbed energy and $E_T(\lambda)$ is the transmitted energy. All these energy types are equal to the total energy which is $E_I(\lambda)$.

These interactions depend on the material type, material temperature and wavelength. This has an important role in distinguishing between surface materials. Even within the same feature type, and because of the wavelength dependency, the proportion of reflected, absorbed, and/or transmitted energy varies at different wavelengths, causing two features which are indistinguishable in one spectral range to be different in another wavelength band. These spectral variations result in the effect of color. (Agouris, 2005)

Reflectance also depends on the geometrical shape of the surface. Reflecting behavior of an object is characterized by the surface roughness in comparison to the wavelength of incident energy.

2.6.1 Specular reflectance

It is of little use in remote sensing because the incoming energy is completely reflected in another direction. (Figure 2.9) Surface particles are small relative to the wavelength. Light is reflected in a single direction and it is also called mirror reflection. Still water, ice and many other minerals with crystal surfaces have the same property and they mostly seen black.

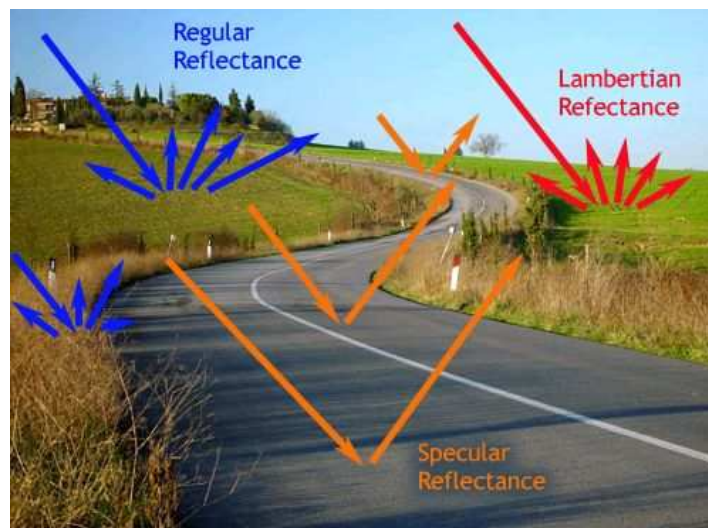


Figure 2.9 Reflectance types

2.6.2 Diffuse reflectance

Diffuse reflections contain spectral information on the colour of the reflecting surface. Remote sensing is mostly interested in measuring the diffuse reflectance properties of terrain features. Surface is rough relative to the incident wavelength. It

is also called isotropic reflection because the energy is reflected equally in all directions (Figure 2.9). Many natural surfaces act as a diffuse reflector to some extent. A perfectly diffuse reflector is termed as Lambertian surface because reflective brightness is same when observed from any angle.

2.6.3 Albedo

The reflectivity of a surface can be measured for a specific wavelength or for the entire electromagnetic spectrum. The spectral reflectance of an object is the percentage of electromagnetic radiance reflected by the object in a specific wavelength or spectral band (Figure 2.10). The albedo of an object is its reflectance aggregated over a broader segment of the electromagnetic spectrum or over the entire spectrum. The higher the albedo, the more reflective the surface and the brighter the surface will appear in remotely sensed imagery. The range can vary from 0 to 100%. Different objects may have similar albedos, measured over a broad portion of the electromagnetic spectrum but may still have very different patterns of reflectance within narrow spectral bands. These differences can be used to discriminate between different types of objects.

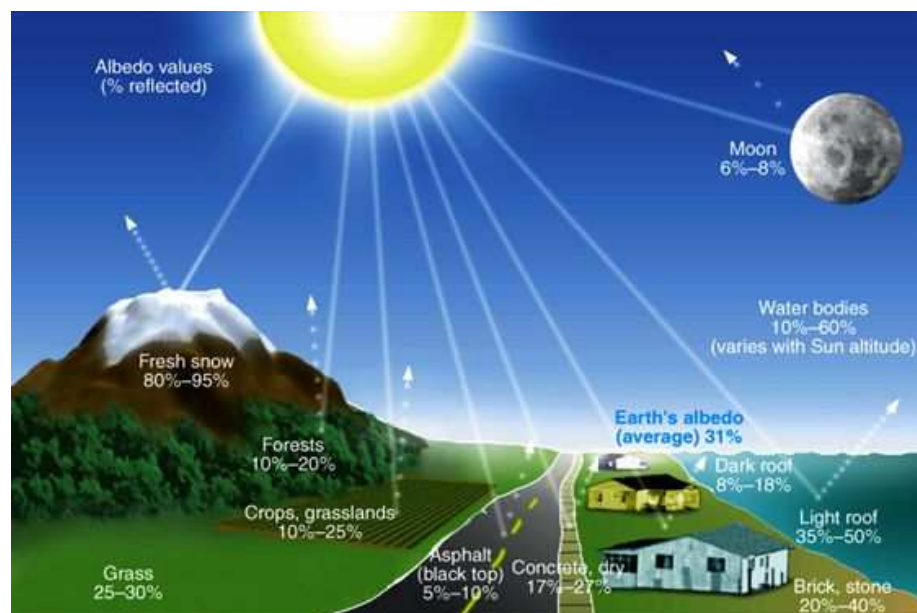


Figure 2.10 Albedo values of different surface materials

2.6.4 Spectral Signatures

Spectral reflectance is the portion of incident radiation that is reflected by a non-transparent surface. The fraction of energy reflected at a particular wavelength varies

for different features. Additionally, the reflectance of features varies at different wavelengths. A spectral signature is a unique reflectance value in a specific part of the spectrum. In order to this two features that are indistinguishable in one spectral range may be very different in another portion of the spectrum. This is an essential property of matter that allows for different features to be identified and separated by their spectral signatures.

Spectral signatures for different surfaces can be obtained using a device called a radiometer. The radiometer detects the electromagnetic radiation reflected off a surface in a specified spectral band. By measuring reflectance in many different bands, the spectral signature over the full range of wavelengths can be obtained.

A spectral reflectance curve is a graph of the spectral reflectance of an object as a function of wavelength and is very useful for choosing the wavelength regions for remotely sensed data acquisition for a certain application (Figure 2.11). (Agouris, 2005)

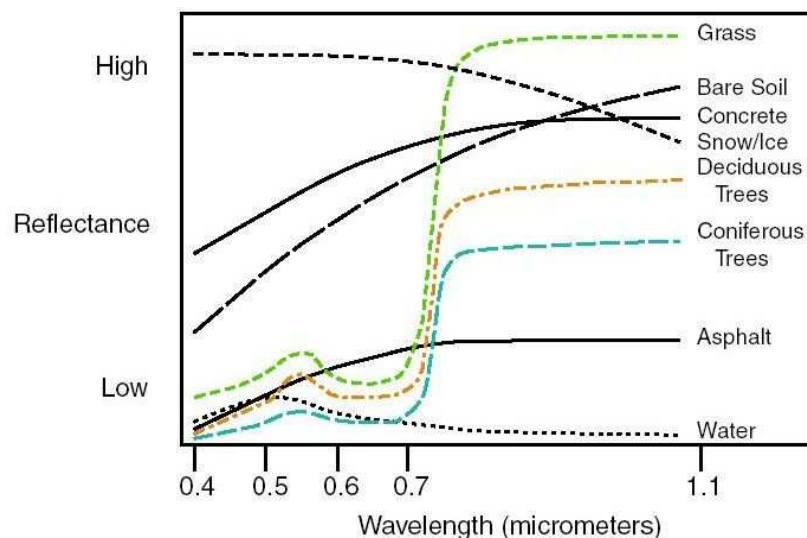


Figure 2.11 Spectral reflectance curves for common cover types

2.7 Spectral Reflectances of Earth Features

The important portion of image analyses is to know and understand the spectral characteristics of features, as well as knowing what factors influence these characteristics. Spectral signatures are used to discriminate features but sometimes it is impossible to distinguish two objects. Because of this the part of the spectrum that must be investigated should be known.

2.7.1 Spectral reflectance of vegetation

There are several factors that influence the reflectance quality of vegetation on satellite and remote sensing images. These include brightness, greenness and moisture. Brightness is calculated as a weighted sum of all the bands and is defined in the direction of principal variation in soil reflectance. Greenness is orthogonal to brightness and is a contrast between the near-infrared and visible bands. It is related to the amount of green vegetation in the scene. Moisture in vegetation will reflect more energy than dry vegetation.

Leaf properties that influence the leaf optical properties are the internal or external structure, such as age, water status, mineral stresses, and the health of the leaf. The reflectance of the optical properties of leaves is the same, regardless of the species. The difference for each leaf is the typical spectral feature recorded for the three main optical spectral domains; leaf pigments, cell structure and water content (Figure 2.12). (Calgary, 2003)

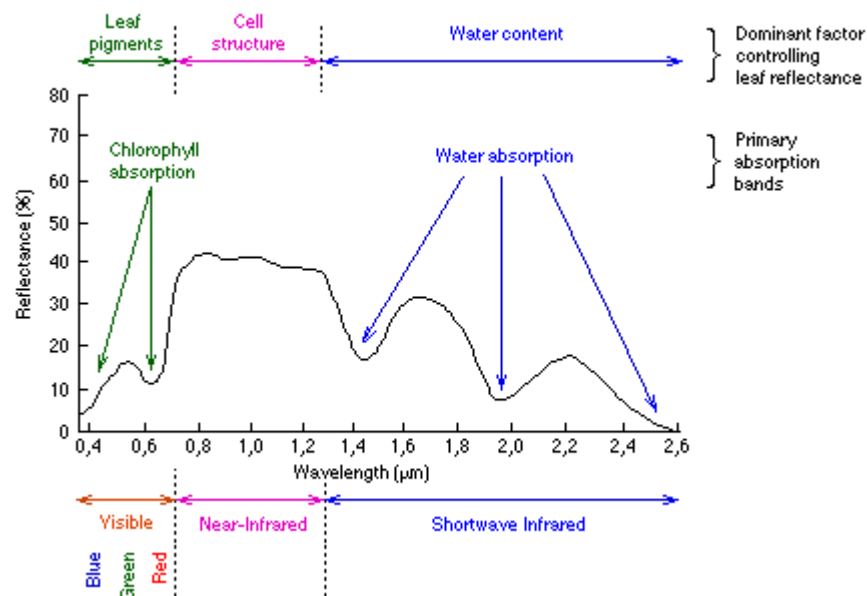


Figure 2.12 Spectral reflectance curve of vegetation (Short, 2007)

The curve shows relatively low values in the red and blue portions of the visible spectrum, with a peak in the green spectral band (Figure 2.12). These features are due to the absorption of blue and red light by chlorophyll. That's the reason of seeing leafs in autumn as yellow or red. Leaf pigments are dominant in the visible wavelength. Generally %70-%90 of blue and red light is absorbed to provide energy

for the process of photosynthesis. There is a slight reflectance peak in green and which is the reason that growing vegetation appears green. The reflection remains high in near infrared region. Cell structures are dominant in near infrared portion and this region is suitable to discriminate the vegetation type. This high reflection coefficient is due to the internal leaf structure. (Mather, 1987)

As the plant grows older the reflection in the near infrared portion decreases whereas the reflectance of visible portion not affected. If there is something wrong with the cell structure this will affect the reflectance and the reflectance will become lesser in unhealthy vegetation type. When the leaf gets thicker the water component will increase relatively and this will also cause less reflection. (Calgary, 2003)

Electromagnetic wavelengths affect different parts of plant and trees. These parts include leaves, stems, stalks and limbs of the plants and trees. The length of the wavelengths also plays a role in the amount of reflection that occurs. Tree leaves and crop canopies reflect more in the shorter radar wavelengths, while tree trunks and limbs reflect more in the longer wavelengths. The density of the tree or plant canopy will affect the scattering of the wavelengths.

The usage of spectral libraries with the adequate remote sensing techniques, it is possible to distinguish different species of vegetation. For example birch, a kind of broad leaf show higher values than pine and fir, evergreen conifer (Figure 2.13).

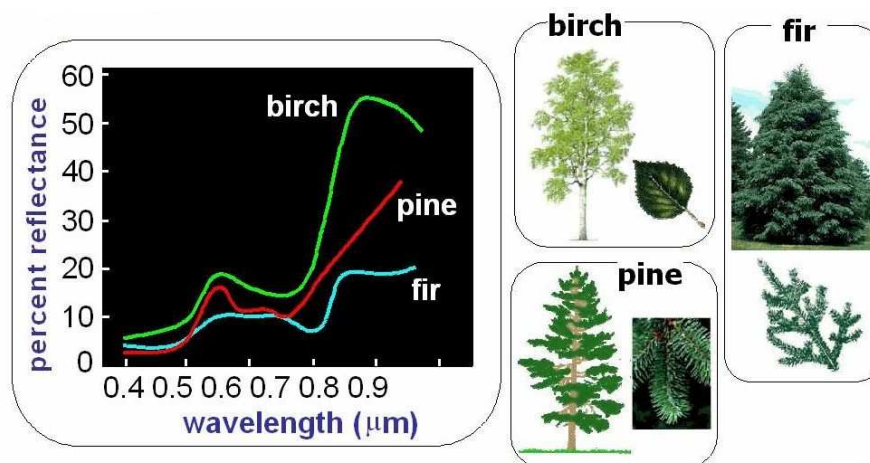


Figure 2.13 Spectral reflectance of different tree species

2.7.2 Spectral reflectance of soil

There are several different areas involved in remote sensing of soils. Satellite imagery will provide the visible boundaries of soil types, while remote sensing will provide for a shallow penetration of soils. Interpreting the remote sensing images and the spectral signatures allow for the classification of the soil types. Air photos and field work measurements provide additional information on soil orders and their relation to vegetation/rock cover, landforms, surficial materials, regional zones, drainage, colour of topsoil, conditions of soil formation and other topographic data.

Main factors that influence the soil reflectance in remote sensing images are mineral composition, soil moisture, organic matter content and soil texture (surface). Size and shape of the soil aggregate also influence the reflectance in the images. Radar waves may not be able to penetrate soil if it is moist. On the soil reflectance spectra, this soil moisture will develop parallel curves. Spectral bands of red and near-infrared bands are independent from the soil moisture. Organic matter may indirectly affect the spectral influence, based on the soil structure and water retention capacity. High organic matter in soil may produce spectral interferences for band characteristics of minerals like Mn and Fe. Soil texture (roughness) also affects soil optical properties. (Calgary, 2003)

2.7.3 Spectral reflectance of water

Remote sensing can be applied to water bodies because energy is absorbed, as well as reflected by water. The reflectance properties of water are a function of the water and the material in the water (organic and/or inorganic material). If the water has a large amount of suspended sediment present, than a higher visible reflectance will result compared to clearer waters. Turbulent water will also affect the amount of energy absorbed and transmitted. The amount of chlorophyll will also affect the amount of water reflectance. An increase in chlorophyll will result in a decrease of blue wavelengths and increase in green wavelengths. Remote sensing can be used to monitor the presence and estimate the concentration of algae. Temperature variations also affect the reflectance of water throughout the day.

Reflectance data for water bodies has been used to detect a number of pollutants (e.g. oil and industrial wastes), and used to determine the presence or absence of tannin dyes from the bog vegetation in lowland areas. (Calgary, 2003)

3 REMOTE SENSING SATELLITES

Remote sensing is observing and measuring our environment from a distance; in order to this the satellite technology has a great role in remote sensing. As the technology advances, use of satellites; that can take photographs of large expanses of land all over the world became available and day-by-day satellites became more efficient. For now, aerial photography has better resolution, with the development of satellite and sensing technologies, satellites will probably have better resolution in the future.

The main advantages of a satellite are;

- Large area coverage;
- Frequent and repetitive coverage of an area of interest;
- Quantitative measurement of ground features using radiometrically calibrated sensors;
- Semiautomatic computerised processing and analysis;
- Relatively lower cost per unit area of coverage.

Each remote sensing satellite has its own altitude, orbit and sensors. Each of these satellites are characterised by the wavelength bands employed in image acquisition, spatial resolution of the sensor, the coverage area and the temporal coverage. Different types of satellite classifications are shown below (CRISP, 2001).

Classification by spatial resolution;

- Low resolution systems (approx. 1 km or more)
- Medium resolution systems (approx. 100 m to 1 km)
- High resolution systems (approx. 5 m to 100 m)

- Very high resolution systems (approx. 5 m or less)

Classification by spectral regions;

- Optical imaging systems (include visible, near infrared, and shortwave infrared systems)
- Thermal imaging systems
- Synthetic aperture radar (SAR) imaging systems

Classification by spectral bands

- Monospectral or panchromatic (single wavelength band, "black-and-white", grey-scale image) systems
- Multispectral (several spectral bands) systems
- Superspectral (tens of spectral bands) systems
- Hyperspectral (hundreds of spectral bands) systems

Classification by combination of frequency bands and polarisation modes used in data acquisition;

- Single frequency (L-band, or C-band, or X-band)
- Multiple frequency (Combination of two or more frequency bands)
- Single polarisation (VV, or HH, or HV)
- Multiple polarisation (Combination of two or more polarisation modes)

3.1 Remote Sensing Satellites for Vegetation Studies

Since different vegetation types have their unique spectral features such as reflectance and emission regions, they can be identified from remote sensing imagery according to their unique spectral characteristics. In the case of vegetation mapping by using remote sensing technology and methodologies, spectral radiances in red and near infrared regions are the handiest among the others. The radiances in these regions could be incorporated into the spectral vegetation indices (VI) that are directly related to the intercepted fraction of photosynthetically active radiation (Xie et al, 2008).

Since different sensors have different spatial, temporal, spectral and radiometric characteristics, the selection of appropriate sensors is very important for mapping vegetation cover. The selection of images acquired by adequate sensors is largely determined by four related factors: (i) the mapping objective, (ii) the cost of images, (iii) the climate conditions (especially atmospheric conditions) and (iv) the technical issues for image interpretation. First, the mapping objective concerns what is to be mapped and what mapping accuracy is expected. In general, images with low resolutions may be adopted only when the high level of vegetation classes are to be identified, while the images with relatively higher resolutions are used for fine-detailed classifications of vegetation. Second, remote sensing imagery may be very expensive and the cost of imagery is definitely a consideration when choosing imagery. From the mapping scale point of view, vegetation mapping at a small scale usually requires high-resolution images, while low-resolution images are used for a large-scale mapping. Third, it raises the issue of the feasibility of using data from different sources to obtain a cloud-free image series over an extended period of time. Lastly, some technical specifics need to be taken into account regarding image quality, preprocessing and interpretation when choosing suitable candidates of sensors (Xie et al, 2008).

The most commonly applied sensors, in the field of vegetation mapping can be considered as Landsat (mainly TM and ETM+), SPOT, MODIS and NOAA–AVHRR among the others (Table 3.1). The general comparison of spectral bands of these satellite systems can be seen in Figure 3.1.

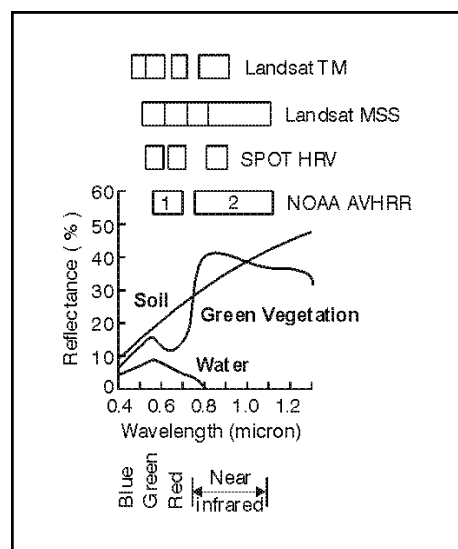


Figure 3.1 Main Earth feature's spectral reflectances in most common satellite bands

Table 3.1 Main features of image products from different sensors (Xie et al, 2008)

Products (Sensors)	Features	Vegetation mapping applications
Landsat TM	Medium to coarse spatial resolution with multispectral data (120 m for thermal infrared band and 30 m for multispectral bands) from Landsat 4 and 5 (1982 to present). Each scene covers an area of 185 x 185 km. Temporal resolution is 16 days.	Regional scale mapping, usually capable of mapping vegetation at community level.
Landsat ETM +	Medium to coarse spatial resolution with multispectral data (15 m for panchromatic band, 60 m for thermal infrared and 30 m for multispectral bands) (1999 to present). Each scene covers an area of 185 km x 185 km. Temporal resolution is 16 days.	Regional scale mapping, usually capable of mapping vegetation at community level or some dominant species can be possibly discriminated.
SPOT	A full range of medium spatial resolutions from 20 m down to 2.5 m, and SPOT VGT with coarse spatial resolution of 1 km. Each scene covers 60 x 60 km for HRV/HRVIR/HRG and 1000 x 1000 km (or 2000 x 2000 km) for VGT. SPOT 1, 2, 3, 4 and 5 were launched in the year of 1986, 1990, 1993, 1998 and 2002, respectively. SPOT 1 and 3 are not providing data now.	Regional scale mapping usually capable of mapping vegetation at community level or species level or global/national/regional scale mapping land cover types (i.e. urban area, classes of vegetation, etc.).
Modis	Low spatial resolution (250–1000 m) and multispectral data from the Terra Satellite (2000 to present) and Aqua Satellite (2002 to present). Revisit interval is around 1–2 days. Suitable for vegetation mapping at a large scale. The swath is 2330 km (cross track) by 10 km (along track at nadir).	Mapping at global, continental or national scale. Suitable for mapping land cover types (i.e. urban area, classes of vegetation, etc.).
AVHRR	1-km GSD with multispectral data from the NOAA satellite series (1980 to present). The approximate scene size is 2400 x 6400 km	Global, continental or national scale mapping. Suitable for mapping land cover types (i.e. urban area, classes of vegetation, water area, etc.).

Ikonos	It collects high-resolution imagery at 1 m (panchromatic) and 4 m (multispectral bands, including red, green, blue and near infrared) resolution. The revisit rate is 3–5 days (off-nadir). The single scene is 11 x 11 km.	Local to regional scale vegetation mapping at species or community level or can be used to validate other classification result.
Quickbird	High resolution (2.4–0.6 m) and panchromatic and multispectral imagery from a constellation of spacecraft. Single scene area is 16.5 x 16.5 km. Revisit frequency is around 1–3.5 days depending on latitude.	Local to regional scale vegetation mapping at species or community level or used to validate vegetation cover extracted from other images.
Aster	Medium spatial resolution (15–90 m) image with 14 spectral bands from the Terra Satellite (2000 to present). Visible to near-infrared bands have a spatial resolution of 15 m, 30 m for short wave infrared bands and 90 m for thermal infrared bands.	Regional to national scale vegetation mapping at species or community level.
Hyperion	It collects hyperspectral image with 220 bands ranging from visible to short wave infrared. The spatial resolution is 30 m. Data available since 2003.	At regional scale capable of mapping vegetation at community level or species level.

3.2 LANDSAT

The LANDSAT program includes a series of optical-infrared remote sensing satellites for land observation (Figure 3.2). Landsat-1 that launched by the USA in 1972 was the first earth observation satellite in the world. Up to now, five Landsat's (Landsat 1-7) have been launched; with only Landsat 5 and 7 still operational LANDSAT-6 was failed to obtain orbit.

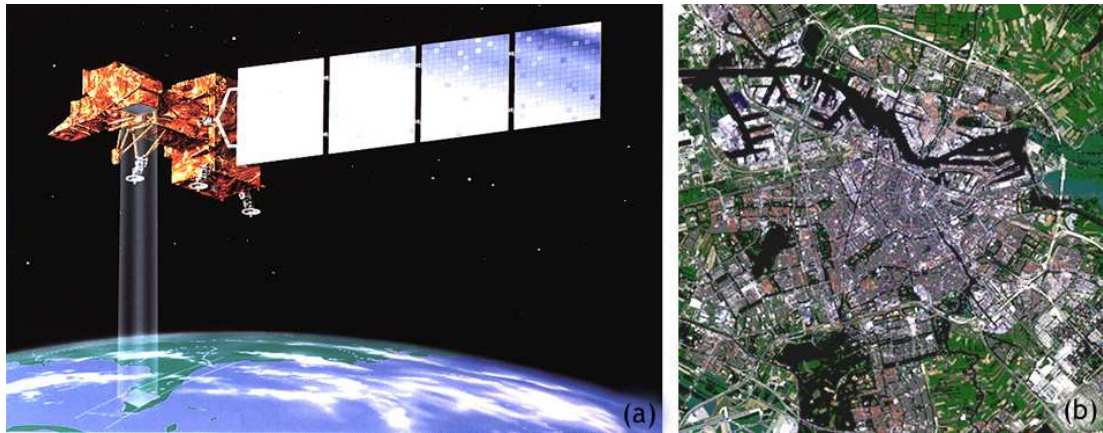


Figure 3.2 (a) Landsat-7 satellite, (b) An example of Landsat-7 scene of Amsterdam

3.2.1 LANDSAT System

- Sensor data acquired: ETM (Enhanced Thematic Mapper);
- Satellite operator: US Geological Survey (USGS);
- Altitude: 705 km;
- Swath width: 185 km;
- Orbit type: near polar, sun-synchronous;
- Orbit period: 99 minutes;
- Repeat cycle: 16 days;
- ETM sensor status: anomaly with Scan Line Corrector, images contain small gaps (GA, 2007).

3.2.2 Sensors

3.2.2.1 MSS (Multi-Spectral Scanner)

MSS sensors scan the earth in lines, which are perpendicular to movement direction of the satellite. MSS had four spectral bands containing red, green, and blue from visible wavelengths and near infrared. The lines are scanned with the help of an oscillating mirror, and six lines are scanned at once at each turn of the mirror.

The resolution of the MSS sensor was 80m. Only the MSS sensor on Landsat 3 had a fifth band in the thermal-IR. Use of MSS was terminated in 1992 (Table 3.2).

Table 3.2 Landsat MSS sensor characteristics

	Band	Wavelength (μm)	Spatial resolution (m)
Green	1	0.5 - 0.6	82
Red	2	0.6 - 0.7	82
Near IR	3	0.7 - 0.8	82
Near IR	4	0.8 - 1.1	82

3.2.2.2 TM (Thematic Mapper)

This sensor is first used in Landsat 4; TM has seven bands from visible (red, green, blue) and infrared (near, short wave, thermal, middle) wavelengths. The resolution is better than MSS; 120m for thermal-IR band and 30m for other bands (Table 3.3).

Table 3.3 TM bands

	Band	Wavelength (μm)	Spatial resolution (m)
Blue	1	0.45 - 0.52	30
Green	2	0.52 - 0.60	30
Red	3	0.63 - 0.69	30
Near IR	4	0.76 - 0.90	30
SWIR	5	1.55 - 1.75	30
Thermal IR	6	10.40 - 12.50	120
SWIR	7	2.08 - 2.35	30

3.2.2.3 ETM+ (Enhanced Thematic Mapper Plus)

ETM+ is carried on board Landsat 7. ETM+ has eighth bands, capable of multispectral scanning. Its spectral bands are similar to the sensors of TM, except that the thermal band (band 6) has an improved resolution of 60 m (versus 120 m in TM). There is also an additional panchromatic band at 15-m resolution (Table 3.4).

Table 3.4 Landsat TM, ETM+ sensor characteristics

	Band	Wavelength (μm)	Spatial resolution (m)
Blue	1	0.45 - 0.52	30
Green	2	0.52 - 0.60	30
Red	3	0.63 - 0.69	30
Near IR	4	0.76 - 0.90	30
SWIR	5	1.55 - 1.75	30
Thermal IR	6	10.40 - 12.50	120 (TM) 60 (ETM+)
SWIR	7	2.08 - 2.35	30
Panchromatic		0.5 - 0.9	15

Landsat 1 had also got a return beam vidicon (RBV) with 3 bands, but due to technical problems that one was never used.

3.2.3 Vegetation and LANDSAT

Landsat data have been applied in vegetation mapping mainly at regional scales. Since Landsat has a long history of dataset, it is very helpful to map long-term vegetation cover and study the spatiotemporal vegetation changes. Because of the different characteristics of spectral sensors (i.e. TM and ETM+) in the Landsat image series, it is necessary to correct the spectral reflectance between images acquired by those sensors. This is especially necessary in long-term vegetation cover monitoring research where both Landsat TM and ETM+ images are used (Xie et al, 2008).

Due to the limitation of spatial resolution, Landsat data is usually used to map vegetation at community level. It is a challenging task to use Landsat images for mapping at species level, especially in a heterogeneous environment. However, when integrating with other ancillary data, it becomes possible to map species (Xie et al, 2008).

The thermal band on Landsat can detect crop health by seeing plants transpire, or lose moisture through their leaves, which is a factor directly related to plant health. When plant transpiration rates decrease in order to this growth rates decrease and the

plants appear unhealthy. Managers use this information to target where to fertilise and irrigate. Other Landsat bands can see the extent of vegetation cover while radar can pick up moisture in the soil.

3.3 SPOT

The SPOT program consists of a series of optical remote sensing satellites. (Figure 3.3) The use of spot is to collect images for land use, agriculture, forestry, geology, cartography, regional planning, water resources and GIS applications. It is committed to commercial remote sensing on an international scale and has established a global network of control centres, receiving stations, processing centres and data distributors. SPOT was first launched in February 1986 by the French Government. There are totally 5 SPOT satellites launched and only SPOT-3 is not operational (CRISP 2001).



Figure 3.3 (a) SPOT 5 satellite, (b) An example of SPOT 5 scene of Amsterdam

3.3.1 SPOT System

- Sensor data acquired: HRV (High Resolution Visible), HRVIR (High Resolution Visible IR) and HRG (High Resolution geometric), HRS (High Resolution Stereoscopic) detectors;
- Satellite operator: French Space Agency, Centre National d'Etude Spatiales (CNES);
- Altitude: 830 km;
- Swath width: 60 km;

- Orbit type: Sun synchronous and semi-recurrent orbit;
- Orbit period: 99 minutes;
- Repeat cycle: 26 days;
- Sensor status: Nominal.

3.3.2 Sensors

3.3.2.1 HRV (High Resolution Visible) and HRVIR (High-Resolution Visible IR) detectors

SPOT has two CCD imageries; HRV (High-Resolution Visible imaging system) sensors with stereoscopic and oblique pointing function. As different from others, SPOT-4 HRVIR, this additionally has a shortwave infrared band. When both sensors are operational, an area of 177km swath wide with 3km area intersected can be acquired in nadir (vertical position). Also every sensor can scan an area independently within ± 27 degrees.

Both HRV and HRVIR have panchromatic and multispectral modes (Table 3.5).

Table 3.5 Spot HRV and HRVIR instrument characteristics (CRISP, 2001)

	Multispectral mode (XS)	Panchromatic mode (P)
Instrument field of view	4.13 deg	4.13 deg
Ground sampling interval (Nadir viewing)	20 m by 20 m	10 m by 10 m
Pixel per line	3000	6000
Ground swath (Nadir viewing)	60 km	60 km

3.3.2.2 HRG (High Resolution Geometric) and HRS (High Resolution Stereoscopic) detectors

It is possible to acquire an image in four different spectral resolution within a 60 km swath with two HRG detectors that were placed on SPOT 5 platform. This detector was designed with the improvements that were made on HRVIR detector.

HRG instrument has a higher ground resolution than that of the HRV/HRVIR on SPOT 1 - 4 satellites: 5 m, and 2.5 m by interpolation in panchromatic mode, and 10 m in all 3 spectral bands in the visible to near infrared ranges. The spectral band in the short wave infrared band is maintained at a resolution of 20 m due to limitations imposed by the geometry of the CCD sensors used in this band (CRISP, 2001). Multispectral bands use CCD sensors comprising 12,000 individual detectors, each measuring $6.5\ \mu\text{m} \times 6.5\ \mu\text{m}$ that have the ability of acquiring images in multispectral while scanning 120 km adjacent area in one pass (SPOT, 2008).

Panchromatic imagery is acquired by sensors comprising two arrays of 12,000 detectors. The same detectors are used on the HRS high resolution stereoscopic instrument. The new HRS instrument acquires images in the panchromatic band only with 10 m spectral resolution. It is designed to acquire images in the panchromatic band at viewing angles of 20° forward and aft of the satellite. It can also obtain stereopair images quickly to generate digital elevation models.

3.3.2.3 Panchromatic (P) mode

Panchromatic mode uses visible part of the electromagnetic spectrum. The panchromatic band in SPOT-1 and SPOT-2 HRV covers 0.51 to $0.73\ \mu\text{m}$. For SPOT-4 HRVIR, the panchromatic band has a narrower bandwidth centred at the red band (0.61 to $0.68\ \mu\text{m}$). Panchromatic mode of SPOT-4 is also known as Monospectral Mode (includes only one spectral band). Either panchromatic or monospectral modes has a 10 m wide pixel and are consist of black-white images. These modes are usually used when examining the geometric details of an area. The panchromatic band of SPOT-5 returns to the values used for SPOT-1 through 3 (CRISP, 2001).

3.3.2.4 Multispectral (XS) mode

Multispectral mode uses three bands; green and red wavelengths of visible portion and near infrared. SPOT-4 has also a forth band which is the short-wave infrared. XS1, XS2 and XS3 denote the three multispectral bands of the HRV (Table 3.6).

Table 3.6 HRV spectral bands

Mode	Band	Wavelength (µm)	Spatial resolution (m)
Multispectral	XS1	0.50 - 0.59 (Green)	20
Multispectral	XS2	0.61 - 0.68 (Red)	20
Multispectral	XS3	0.79 - 0.89 (Near IR)	20
Panchromatic	P	0.51 - 0.73 (Visible)	10

XI1, XI2, XI3 and XI4 denote four multispectral bands in HRVIR (Table 3.7). By combining the data recorded in these bands, colour composite images can be produced with a pixel size of 20 meters.

Table 3.7 HRVIR spectral bands

Mode	Band	Wavelength (µm)	Spatial resolution (m)
Multispectral	XI1	0.50 - 0.59 (Green)	20
Multispectral	XI2	0.61 - 0.68 (Red)	20
Multispectral	XI3	0.79 - 0.89 (Near IR)	20
Multispectral	XI4	1.53 - 1.75 (SWIR)	20
Monospectral	M	0.61 - 0.68 (Red)	10

In order to ensure continuity with the SPOT 1-4 satellites, the SPOT-5 spectral bands are same as those for SPOT-4 (Table 3.8) (CRISP, 2001).

Table 3.8 HRG spectral bands

Mode	Band	Wavelength (µm)	Spatial resolution (m)
Multispectral	1	0.50 - 0.59 (Green)	10
Multispectral	2	0.61 - 0.68 (Red)	10
Multispectral	3	0.79 - 0.89 (Near IR)	10
Multispectral	4	1.53 - 1.75 (SWIR)	20
Monospectral	P	0.51 - 0.73 (Visible)	5 m (2.5 m by interpolation)

3.3.2.5 Supermode

Supermode is a unique image sampling process that improves resolution in the panchromatic band without major modifications to the satellite. The Supermode process generates a single image at a resolution of 2.5 metres from two panchromatic images acquired simultaneously at a resolution of 5 metres and offset vertically and horizontally by 2.5 metres. Imagery is acquired by two dedicated arrays of CCD detectors offset in the focal plane.

In the first step of the supermode the instrument generates two 5-metre images that are processed independently by the payload. Then interpolation, deconvolution and noise removal processes are applied in order to obtain the 2.5 m image of the area (Figure 3.4).

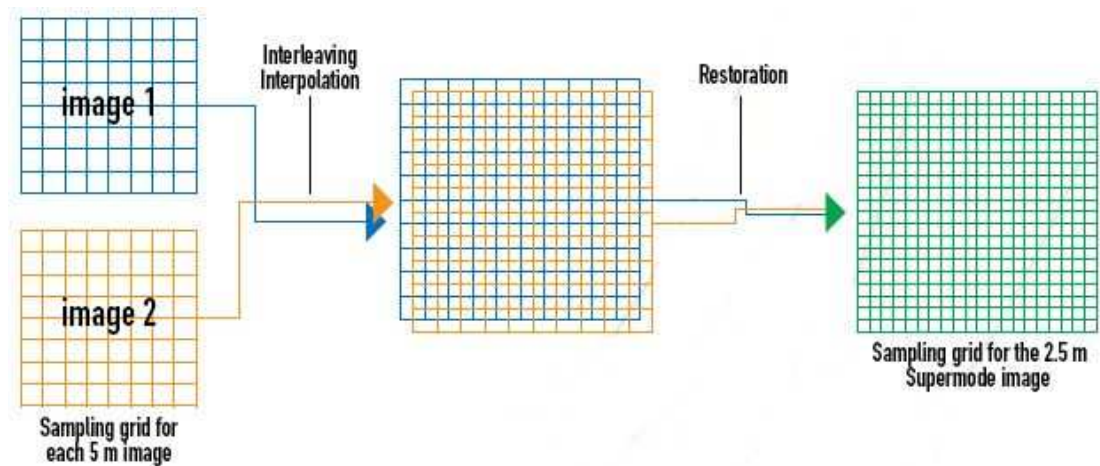


Figure 3.4 SPOT 5 Supermode processess

3.3.3 Vegetation and SPOT

Due to the multiple sensor instruments and the revisit frequencies, SPOT satellites are capable of obtaining an image of any place on earth every day and having an advantage of mapping vegetation at flexible scales (regional, national, continental or global).

The SPOT-4 and -5 satellites carry a low-resolution wide-coverage instrument that are very useful for observing and analyzing the evolution of land surfaces and understanding land changes over large areas. Vegetation-2 instrument that is located on SPOT-5 satellite is identical to the instrument on SPOT-4, with some enhancements to critical technologies such as sensors and optical coatings. The instrument has resolution of 1 km with a swath of 2250 km. The wide imaging swath

helps the Vegetation instrument cover almost all of the globe's landmasses in a single day. It observes landmasses during the daytime and stops imaging when the satellite passes over the oceans. The instrument gathers light reflected by the Earth's surface and transforms it into discrete pixel values (CNES, 2008).

3.4 NOAA/AVHRR

National Oceanic and Atmospheric Administration's (NOAA's) Polar Orbiting Environmental Satellites (POES) began with TIROS-N in 1978 (Figure 3.5). At the moment, five satellites are operational; NOAA-9, 10, 14, 17, 18.

The AVHRR is a broad band, four or five-channel scanner, using the visible, near infrared, and thermal infrared portions of the electromagnetic spectrum.

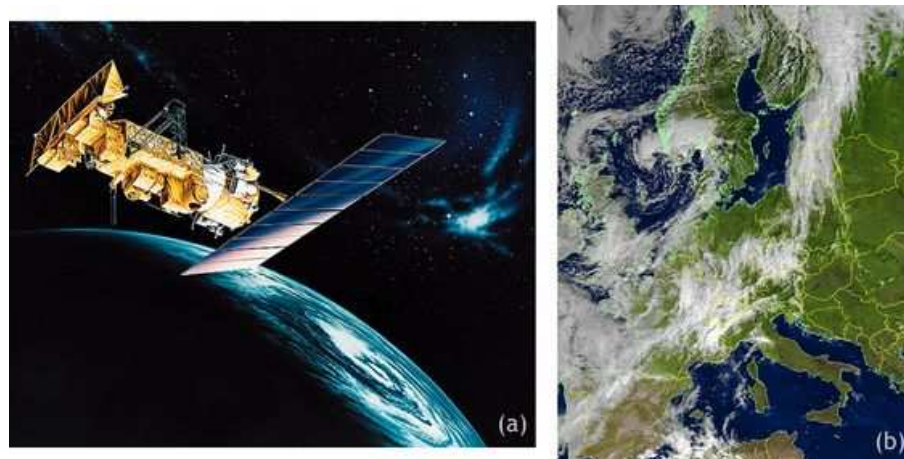


Figure 3.5 (a) NOAA satellite, (b) An example of NOAA-17 scene of Europa

3.4.1 AVHRR System

- Sensor data acquired: AVHRR;
- Satellite operator: NOAA;
- Altitude: 850 km;
- Swath width: up to 3000 km;
- Orbit type: near polar, sun-synchronous;
- Orbit period: 101.2 minutes;
- Repeat cycle: 9 days at nadir;
- AVHRR Sensor Status: Nominal (GA, 2007).

3.4.2 Sensors

In a day, the satellite can take at least four images of any area on the earth. One of the main instruments carried on the satellite is the AVHRR (Advanced Very High Resolution Radiometer) for observation of clouds and land and sea surface at 1 km resolution in the total of five bands in visible and infrared wavelength regions (Table 3.9).

Table 3.9 AVHRR sensor characteristics (CRISP, 2001)

	Band	Wavelength (μm)	Applications
Visible	1	0.58-0.68	Cloud, snow and ice monitoring
Near IR	2	0.725-1.10	Water, vegetation and agriculture surveys
Short Wave IR	3A	1.58-1.64	Snow, ice and cloud discrimination
Medium Wave IR	3B	3.55-3.93	Sea surface temperature, volcano, forest fire activity
Thermal IR	4	10.3-11.3	Sea surface temperature, soil moisture
Thermal IR	5	11.3-12.5	Sea surface temperature, soil moisture

Also, the satellites after NOAA 14, have an another band; short-wave infrared, but five of these are active at a time. AVHRR data are acquired in three formats: High Resolution Picture Transmission (HRPT), Local Area Coverage (LAC), and Global Area Coverage (GAC).

HRPT data are full resolution image data transmitted to a local ground station as they are being collected. LAC are also full resolution data, but recorded with an on-board tape recorder for subsequent transmission during a station overpass. GAC data provide daily subsampled global coverage recorded on the tape recorders and then transmitted to a ground station (CRISP, 2001).

3.4.3 Vegetation and NOAA/AVHRR

AVHRR has an image archive with long history (ever since 1978 when the first AVHRR was launched), it is very useful to study long-term changes of vegetation.

AVHRR image data have two spatial resolutions: ~1.1 km for local area coverage (LAC) and 5 km for global area coverage (GAC). These are both widely used to study and monitor vegetation conditions in ecosystems, including forests, tundra, grasslands, agricultural lands, land cover mapping and production of large-scale maps for these subjects. One of the obvious advantages of AVHRR is the low cost and the high probability of obtaining a cloud-free view of the land surface. In addition, GLCC (Global Land Cover Characterization) was produced based on AVHRR image data (Xie et al, 2008).

In AVHRR, data from the visible (Channel 1) and near infrared (Channel 2) channels are combined into a ratio, the Normalized Difference Vegetation Index. The AVHRR-NDVI has been widely used in various operational applications, including famine early warning systems, land cover classification, health and epidemiology, drought detection, land degradation, deforestation and in relating large-scale interannual variations in vegetation to climate (Didan, 2003).

AVHRR imagery have certain limitations in calibration, geometry, orbital drift, limited spectral coverage and variations in spectral coverage especially in the early period of applications. Its utility has been restricted because its use often introduces substantial errors at various stages of processing and analysis.

Nevertheless, many projects including GLCC, aiming at mapping vegetation covers at continental to global scales have been carried out using AVHRR for years simply depending on its low cost and easy access (Xie et al, 2008).

3.5 MODIS

The Moderate-resolution Imaging Spectroradiometer (MODIS) is an instrument found in two satellites; Terra (launched in 1999) and Aqua (launched in 2002) (Figure 3.6). Terra MODIS and Aqua MODIS are viewing the entire Earth's surface every 1 to 2 days, acquiring data in 36 spectral bands, or groups of wavelengths.



Figure 3.6 (a) Aqua satellite, (b) Terra satellite, (c) An example of Terra/Modis scene of Netherlands

3.5.1 Terra MODIS System

- Sensor data acquired: MODIS (Moderate-Resolution Imaging Spectroradiometer);
- Satellite operator: NASA;
- Altitude - at equator: 705 km;
- Swath width: 2300 km;
- Orbit type: near polar, sun-synchronous;
- Orbit period: 96.5 minutes;
- Repeat cycle: 16 days;
- MODIS sensor status: Nominal (GA, 2007).

3.5.2 Aqua MODIS System

- Sensor data acquired: MODIS (Moderate-Resolution Imaging Spectroradiometer);
- Satellite operator: NASA;
- Altitude - at equator: 705 km;
- Swath width: 2330 km;

- Orbit type: near polar, sun-synchronous;
- Orbit period: 98.8 minutes;
- Repeat cycle: 16 days;
- MODIS sensor status: Nominal (GA, 2007).

MODIS provides high radiometric sensitivity (12 bit) in 36 spectral bands between wavelengths; 0.4 μm and 14.4 μm . Two of these bands' resolution is 250 m, another five bands have 500 m resolution and the rest twenty-nine bands have a resolution of 1km. The Scan Mirror Assembly uses a continuously rotating double-sided scan mirror to scan ± 55 degrees. The optical system consists of a two-mirror off-axis, a focal telescope, which directs energy to four refractive objective assemblies; one for each of the VIS, NIR, SWIR/MWIR and LWIR spectral regions to cover a total spectral range of 0.4 to 14.4 μ (Maccherone, 2007). Bands 1 to 19 are in nm; Bands 20 to 36 are in μm .

3.5.3 Vegetation and MODIS

MODIS has two vegetation indexes that are produced globally over land at 1 km and 500 m resolutions and 16-day compositing periods; NDVI (Normalized Difference Vegetation Index) and EVI (Enhanced Vegetation Index). Whereas the NDVI is chlorophyll sensitive, the EVI is more responsive to canopy structural variations, including LAI (Leaf Area Index), canopy type, plant physiognomy, and canopy architecture. The MODIS NDVI is referred to as the "continuity index" to the existing 20+ year NOAA-AVHRR derived NDVI time series (Didan, 2003).

**The atmospherically corrected reflectances of MODIS bands 1 and 2 are
directly input into the NDVI equation (Table 3.10 -**

Table 3.11). For the EVI, band 3 will also be utilized (Didan, 2003).

Table 3.10 MODIS Band 1-19 sensor characteristics

Primary Use	Band	Bandwidth (nm)	Spatial resolution (m)
Land/Cloud/Aerosols Boundaries	1	620-670	250
	2	841-876	250
Land/Cloud/Aerosols Properties	3	459-479	500
	4	545-565	500
	5	1230-1250	500
	6	1628-1652	500
	7	2105-2155	500
Ocean Color Phytoplankton Biogeochemistry	8	405-420	1000
	9	438-448	1000
	10	483-493	1000
	11	526-536	1000
	12	546-556	1000
	13	662-672	1000
	14	673-683	1000
	15	743-753	1000
	16	862-877	1000
Atmospheric Water Vapour	17	890-920	1000
	18	931-941	1000
	19	915-965	1000

Table 3.11 MODIS Band 20-36 sensor characteristics

Primary Use	Band	Bandwidth (μm)	Spatial resolution (m)
Surface/Cloud Temperature	20	3.660-3.840	1000
	21	3.929-3.989	1000
	22	3.929-3.989	1000
	23	4.020-4.080	1000
Atmospheric Temperature	24	4.433-4.498	1000
	25	4.482-4.549	1000
Cirrus Clouds Water Vapour	26	1.360-1.390	1000
	27	6.535-6.895	1000
	28	7.175-7.475	1000
Cloud Properties	29	8.400-8.700	1000
Ozone	30	9.580-9.880	1000
Surface/Cloud Temperature	31	10.780-11.280	1000
	32	11.770-12.270	1000
Cloud Top Attitude	33	13.185-13.485	1000
	34	13.485-13.785	1000
	35	13.785-14.085	1000
	36	14.085-14.385	1000

4 DIGITAL IMAGE PROCESSING

Image is a representation, likeness or imitation of an object or thing, a vivid graphic description; something introduced to represent something else. The word “digital” is a term related to representation by numbers, numerical methods, in computers. A digital image is as a numerical representation of an object in which the pixels are discrete units and integer gray scale supplies the numerical component (Figure 4.1). Processing is the operations to get the desired result. According to the definitions; “digital image processing” can be described as a set of operations on a numerical representation of an object or a thing in order to obtain a desired result (Lillesand, 1987).

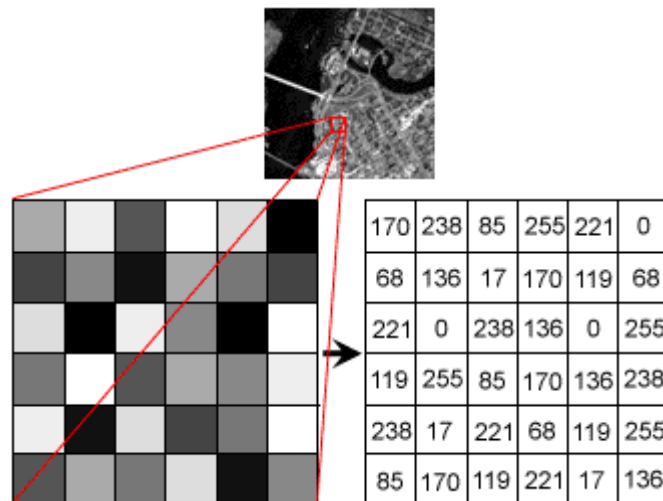


Figure 4.1 Digital image representation

4.1 Image Resolution

The characteristics of a remote-sensing instrument operating in the visible and infrared spectral bands are described in terms of its spatial, spectral, radiometric and temporal resolution.

The analysts have to know the resolutions in order to have exact meaningful biophysical or hybrid information from remotely sensed imagery.

4.1.1 Spatial Resolution

Spatial resolution is the smallest unit of an image and is measured by a pixel (picture element). It's the amount of area covered by a single pixel, an ability to separate two different objects from each other. A spatial resolution of 10 meters means that an individual pixel represents an area on the ground of 10 meters by 10 meters. Thus any objects, which are smaller than 10 meters, will not be distinguishable in the image (Figure 4.2). A high spatial resolution (1-2 meters) remotely sensed data is very useful for agricultural applications where within field variability is studied. Low spatial resolution (20-30 meters) has limited the use of satellite imagery and encouraged the development of a new generation of land observation satellites to be launched.



Figure 4.2 Toulouse, viewed at different resolutions by SPOT Image satellites

(a) 20 m, (b) 10 m, (c) 5 m, (d) 2.5 m

One practical limit to resolution is the capacity of the recording system to handle the data. Higher resolution covers large amount of data. For example, a single band of a TM image of an area 90km x 90km will contain about 9 million pixels whereas an image of the same area from the new Indian satellite will contain about 324 million pixels. (Figure 4.3) Another limit is the strength of the signal, which can be recorded. There are a number of factors that control the signal strength. But the basic consideration is that there always some background noise in the system and the sensor needs to be able to record the signal so that it is always considerably stronger than this noise (Lillesand, 1987).

When remotely sensed data are acquired by a sensor system at the same IFOV (Instantaneous Field of View), registration is much easier and more accurate. If IFOV is different between the two images, resample to a uniform pixel size. Two images with significantly different look angles can cause problems when used for change detection purposes. Differences in reflectance from the two data sets may cause spurious change detection results.

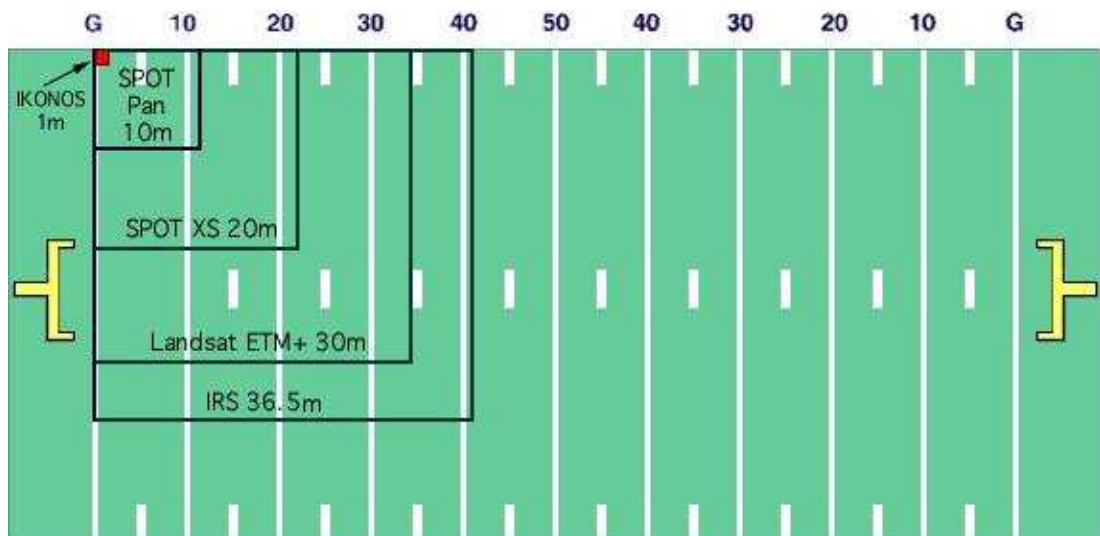


Figure 4.3 Differences in spatial resolution among some well known sensors

4.1.2 Spectral Resolution

Remote sensing systems make measurements in more than one band in electromagnetic spectrum. Spectral resolution can be explained in two ways; first is the spectral bandwidth. It isn't possible to have thousands of measurements for single wavelength. So, any real measurement is the weighted average over some range of wavelengths. When the bandwidth is narrower, the spectral resolution gets better

(Figure 4.4). For example a sensor, which can measure over a $0.05 \mu\text{m}$ interval, has a fine spectral resolution. Detecting over a broad wavelength band of the electromagnetic spectrum such as a 35 mm camera using colour film, has a coarse spectral resolution as the film records the entire visible spectrum (UTEP, 2002).

Second is the number of bands. For example, TM data with measurements in 7 bands clearly has less resolution than MODIS data with measurements in 36 bands. In this situation, data size marks the limits. On the other hand the basic thing is to make it possible to identify materials based on their spectral reflectance curves. Systems such as MODIS have been given the name hyperspectral, but they are like any other system except for the number of bands for which data are available.

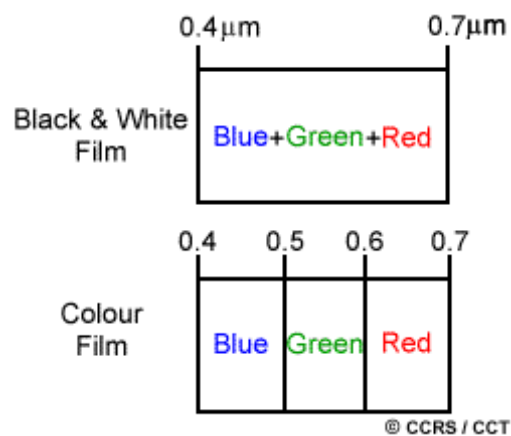


Figure 4.4 The comparison between the colour film and the black and white film

The data acquired on multiple dates from the same sensor system in the same bands achieves best results. When this is not possible, bands that most closely approximate one another should be used.

4.1.3 Radiometric Resolution

Radiometric resolution is the number of digital levels used to express the data collected by the sensor. All sensors convert received radiation into a digital form, which consists of a number that falls within some range of values. Radiometric resolution defines this range of values. A sensor with 8-bit resolution (Landsat TM) has a range of 256, or 2^8 , values. A 12-bit sensor (SPOT Panchromatic) has a range of 4096, or 2^{12} , values (Figure 4.5). Radiometric resolution can be thought of as the sensor's ability to make fine or subtle distinctions between reflectance values

When the radiometric resolution of data acquired by one system is compared with data acquired by a higher radiometric resolution instrument (e.g., Landsat TM with 8-bit data) then the lower resolution data (e.g., 6-bit) should be decompressed to 8-bits for change detection purposes. However, the precision of decompressed brightness values can never be better than the original, uncompressed data.

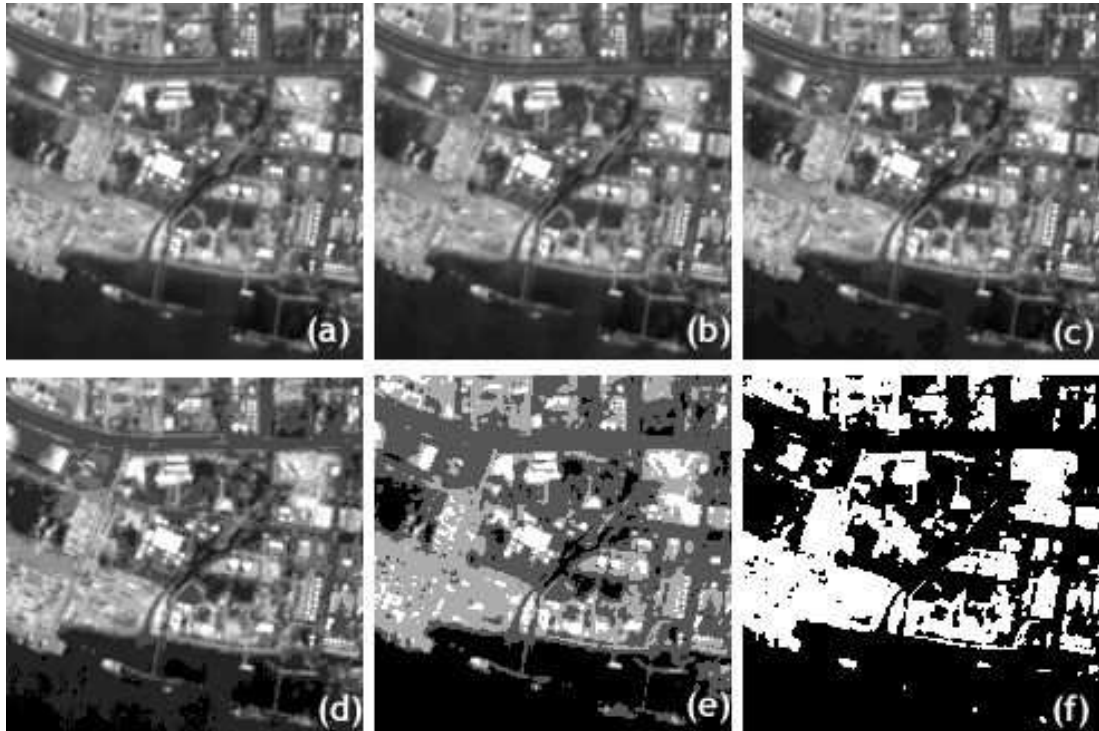


Figure 4.5 Spot Panchromatic images with different radiometric resolutions; (a) 8 bit quantization - 256 levels, (b) 6 bit quantization - 64 levels, (c) 4 bit quantization - 16 levels, (d) 3 bit quantization - 8 levels, (e) 2 bit quantization - 4 levels, (f) 1 bit quantization - 2 levels

4.1.4 Temporal Resolution

Temporal resolution is a measure of how often the same area is visited by the sensor. For example, Landsat TM has a temporal resolution of 16 days, while AVHRR data is collected once per day. Temporal resolution does not describe a single image, but rather a series of images as the same sensor captures them over time. The temporal resolution of satellite imagery depends on the satellites orbit characteristics; aerial photography obviously requires special flight planning for each acquisition.

Temporal resolution is a problem that can be associated with satellite imagery. For example, in farming systems where there is constant change during a growing season

the time between satellite revisits has not been frequent enough for crop monitoring. On the other hand airborne systems have flexibility when scheduling flyovers, however weather conditions are limiting airborne systems.

4.2 Preprocessing

Preprocessing involves the correction of distortion, degradation, and noise introduced during the imaging process. The aim of preprocessing is to produce a corrected image that is as close as possible, both geometrically and radiometrically, to the radiance characteristics of the original scene.

4.2.1 Geometric Corrections

Digital images collected from airborne or spaceborne sensors often contain systematic and unsystematic geometric errors. Some of these errors can be corrected by using ephemeris of the platform and known internal sensor distortion characteristics. Other errors can only be corrected by matching image coordinates of physical features recorded by the image to the geographic coordinates of the same features collected from a map or GPS.

Geometric errors that can be corrected using sensor characteristics and ephemeris data include scan skew, mirror-scan velocity variance, panoramic distortion, platform velocity, and perspective geometry (systematic). Errors that can only be accounted for by the use of GCP's include the roll, pitch, and yaw of the platform and/or the altitude variance (USG, 1998).

- Image to Ground Geocorrection: The correction of digital images to ground coordinates using GCP collected from maps or ground GPS reconnaissance.
- Image-to-Image Geocorrection: Image to image correction involves matching the coordinate systems of two digital images with one image acting as a reference image and the other as the image to be rectified

4.2.1.1 Image Resampling Methods

- Nearest Neighbour: Uses the input cell value closest to the output cell as the assigned value to the output cell

- Bilinear Interpolation: Calculates the output cell value by calculating the weighted average of the four closest input cells (a 2 x 2 array) based on distance.
- Cubic convolution: Calculates the output cell value by calculating the weighted average of the closest 16 input cells (a 4 x 4 array) based on distance.

4.2.2 Radiometric Corrections

The main purpose for applying radiometric corrections is to reduce the influence of errors or inconsistencies in image brightness values; as referred to noise, that may limit one's ability to interpret or quantitatively process and analyse digital remotely sensed images. Radiometric noise generated by remote sensing instruments can take the form of random brightness deviations from electrical sources and coherent radiation interactions or more systematic variations that have spatial structure or temporal persistence.

The causes of radiometric noise are; changes in scene illumination, changes in atmospheric conditions, viewing geometry and instrument response characteristics. For radiometric correction, combine images from different dates and/or adjacent tracks are needed.

Types of corrections are;

- Sun elevation corrections
- Earth-sun distance corrections
- Haze compensations
- Conversion to absolute radiance

4.3 Image Ratio

Image rationing is commonly used as a vegetation index, to remove the variable effects of topography or to emphasise certain surface chemicals evident for vegetation free rocks and soils. This can be done by dividing the digital numbers of one image band by those of another image band and creating a third image. Ratio images may also be used to remove the influence of light and shadow on a ridge due to the sun angle. It is also possible to calculate certain indices that can enhance vegetation or geology.

4.3.1 Normalized Difference Vegetation Index (NDVI)

NDVI is the acronym for normalised difference vegetation index.

$$\text{NDVI} = (\text{near IR band} - \text{red band}) / (\text{near IR band} + \text{red band}) \quad (4.1)$$

$$\text{NDVI} = (\text{NIR} - \text{VIS}) / (\text{NIR} + \text{VIS}) \quad (\text{if no red band exist})$$

The differential reflectance in these bands provides a means of monitoring density and vigour of green vegetation growth using the spectral reflectivity of solar radiation. Chlorophylls, the pigments in green plants absorb light primarily from the red and blue portions of the spectrum, while a higher proportion of infrared is reflected or scattered. NDVI tends to increase with increases in green leaf biomass or leaf area index. Rock and bare soil have similar reflectance in the red and the near infrared, so these surfaces will have values near zero. Green leaves commonly have larger reflectance in the near infrared than in the visible range. As the leaves come under water stress, become diseased or die, they become more yellow and reflect significantly less in the near infrared range. NDVI can be used as an indicator of relative biomass and greenness. If sufficient ground data is available, the NDVI can be used to calculate and predict primary production, dominant species, and grazing impact and stocking rates (NRRI, 2000).

Green leaves have a reflectance of 20 percent or less in the 0.5 to 0.7-micron range (green to red) and about 60 percent in the 0.7 to 1.3-micron range (near infrared). The result is always between -1 and 1, in which -0,1 means not a green area and 0,6 is a very green area.

However, dust and aerosols can cause errors; Rayleigh scattering, subpixel-sized clouds. Near to these, large solar zenith angles and large scan angles increase red band with respect to near IR band and reduce the computed NDVI. So a preprocessing to decrease these effects is needed, but even after a preprocessing NDVI is still sensitive to external factors such as soil background that are most obvious in areas with sparse vegetation. Also NDVI is only sensitive to the green vegetation and might not recognise non-photosynthetic vegetation.

4.3.2 Difference Vegetation Index (DVI)

DVI is sensitive to the amount of vegetation. Generally used for distinguishing soil and vegetation, but DVI doesn't deal with the difference between reflectance and radiance caused by the atmosphere or shadows, so it can't distinguish vegetation from soil in shady areas very well due to a problem caused by topography. The DVI is performed with the formula given below.

$$\text{DVI} = \text{NIR} - \text{R} \quad (4.2)$$

Where NIR and R represents the Near-infrared and Red bands respectively.

4.3.3 Soil Brightness Index (SBI)

Soil brightness index indicates bare areas such as agricultural fields, beaches, parking lots as the lightest features whereas agricultural fields with harvest and forests as the darkest features within the image. The soil brightness index for SPOT-5 is performed using the following formula (Lau et al 1998);

$$\text{BRIGHTNESS} = 0.60539 \times \text{Band1} + 0.61922 \times \text{Band2} + 0.50008 \times \text{Band3} \quad (4.3)$$

4.4 Change Vector Analysis (CVA)

Change vector analysis (CVA) is a robust approach for detecting and characterizing radiometric change in multispectral remote sensing data sets. CVA is reviewed as a useful technique to:

- Process the full dimensionality of multispectral/multi-layer data so as to ensure detection of all change present in the data;
- Extract and exploit the components of change in multispectral data;
- Facilitate composition and analysis of change images (Johnson & Kasischke, 1998).

Change vector analysis (CVA) is a radiometric technique, the primary utility of which is the detection of all changes present in the input multispectral data (Malila, 1980). The method is also exible enough to be active when using diverse types of sensor data and radiometric change approaches, and it is capable of incorporating categorical information as well.

The potential advantages of CVA over some other methods can be considered as:

- Capability to concurrently process and analyse change in all multispectral input data layers (as opposed to selected bands);
- Avoidance of compounding of spatial-spectral errors often inherent in multi-date classifications;
- Capability to detect changes both in land cover and condition;
- Computation and separation of multidimensional change vector components, and composition of change images that retain this information and facilitate change interpretation and labeling (Johnson & Kasischke, 1998).

There are also other change detection approaches possibly implemented digitally. The choice of the available techniques was based on different factors given in below;

Table 4.1 Factors in choice of the CVA Approach (Malila, 1980)

Factor	Advantages of CVA technique	Advantages of other techniques
Choice of pixel groups as analysis units rather than individual pixels	<ul style="list-style-type: none"> • Reduced number of units to be analysed • Choice of min. size • Stand-like units defined in common • Large reduction of salt and pepper effect in map products • Reduce effect of noise due to averaging • Reduced sensitivity to spatial misregistration 	<p>Individual pixels:</p> <ul style="list-style-type: none"> • One pass through data instead of two, except additional pass required for spatial processing • Finer spatial detail
Omission of classification	<ul style="list-style-type: none"> • Elimination of errors due to misclassification • Much reduced ground truth and training requirements • Reduced sensitivity to topographic effects 	<p>Classification:</p> <ul style="list-style-type: none"> • Classification step may be required later
Analyses of change vectors rather than data differences	<ul style="list-style-type: none"> • More complete use of information • Interpretability and quantification of change direction and magnitude • Availability of information for later identification and mensuration 	<p>Data differencing:</p> <ul style="list-style-type: none"> • Faster • Lower cost

However, like other radiometric change approaches, CVA also has drawbacks that limit its use. These include;

- A strict requirement for reliable image radiometry: Because CVA is based on pixel-wise radiometric comparison, the accuracy of image radiometric correction for alleviating the impacts caused by disturbing factors such as different atmospheric conditions, solar angle, soil moisture and vegetation phenology, etc., is more critical for CVA than for spectral classification approaches. However, there exists no valid radiometric correction method that can be used to reduce the effects of all disturbing factors efficiently, especially for vegetation phenology. Similar acquisition dates in different years could be therefore chosen to reduce this type of disturbance in CVA (Chen et al, 2003).
- A lack of automatic or semiautomatic methods to effectively determine the threshold of change magnitude between change and no-change pixels: Although determination of the optimal threshold between change and non-change pixels is considered as the most important task as well as the greatest challenge of CVA (Ding et al, 1998; Johnson & Kasischke, 1998; Smits & Annoni, 2000), the threshold in a specific CVA analysis is often determined according to empirical strategies (Fung & Le-Drew, 1988) or from manual trial-and-error procedures. This usually requires a more experienced image analyst and a long trial time (Bruzzone & Prieto, 2000).
- Discrimination of different phenomenological types of change is problematic when the number of bands involved is large: The methods of discriminating change type in existing literature can be grouped into three classes: (1) trigonometric functions of vector angle in two spectral dimensions (Malila, 1980), (2) sector coding in more than two spectral dimensions (Virag and Colwell, 1987), and (3) principal component analysis in a multitemporal space (Lambin and Strahler, 1994a). In most CVA applications the change category is mainly distinguished and assigned by a combination of “+” or “-” symbols (+ for increase, - for decrease) of each computational band and image interpretation (Virag & Colwell, 1987; Michalek et al., 1993; Johnson & Kasischke, 1998; Sohl, 1999).

CVA is a multivariate technique, that accepts as input of n bands, from each multitemporal scene pair. After the geometrically registration and radiometrically normalization of the corresponding input bands from each acquisition, CVA may be implemented. The CVA algorithm produces two 'channels' of output change information: (1) change vector direction; and (2) multispectral change magnitude (Figure 4.6). Changed areas can then be described in these terms, as well as by other attributes such as geographic location and area.

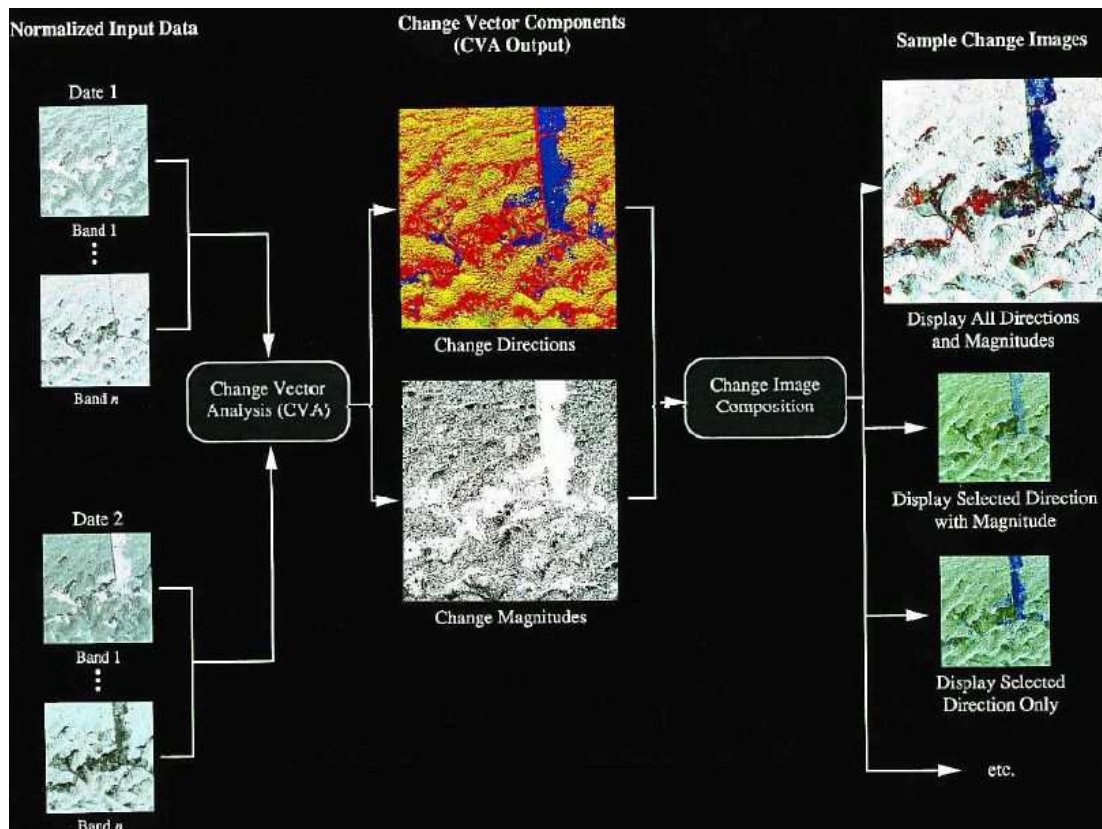


Figure 4.6 Flow diagram of CVA based change detection
(Johnson & Kasischke, 1998)

In CVA technique, a change pixel supposed to be plotted with two different points representing the digital number values of two different acquisition dates. These points should be essentially at the same position on both dates for an unchanged pixel observation which is subject to noise and normalization error (Figure 4.7). The relation of the change where occurred can be characterized by a change vector with a measurable direction and magnitude.

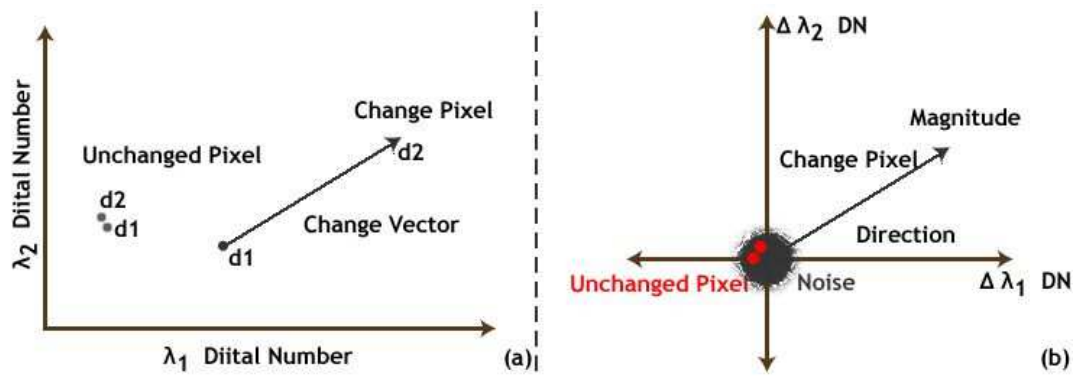


Figure 4.7 Representation of change vector in 2-band (a) radiometric space, (b) radiometric change space

Unchanged pixels actually fall within a volume about the origin due to factors such as noise and imperfect normalization. This 'noise' is generally removed from further consideration by applying a threshold to the magnitude channel.

The potentially large number of possible change vector directions is often desirable to implement some type of simplification in the characterization of change direction. This has been accomplished in a number of ways that vary in complexity and ease of implementation (Johnson & Kasischke, 1998). In this study the numbers of pixels taking part in different directions were used to define the amount of deforestation, forestation and areas with no change.

CVA is an important utility in situations where full-dimensional radiometric change information is desired or required. Such cases include those in which: (1) all changes in terrain type and condition are potentially of interest; or (2) all changes must first be detected before it is possible or appropriate to separate changes of interest; or (3) the subset of changes of interest is known *a priori*, but the optimal spectral metrics for reliable detection of these changes are not known (Johnson & Kasischke, 1998).

Change vector direction is an useful aid in discrimination of different phenomenological types of change, and change magnitude is useful for relative comparisons within and among change types (Johnson & Kasischke, 1998).

4.4.1 Preprocessing requirements of CVA

The most critical pre-processing requirements for CVA are the accurate geometric registration and radiometric normalization of the input data.

Image-to-image registration quality is critical in change detection. Misregistration will lead to change detection commission errors that will corrupt results, and are extremely difficult or impossible to mitigate via post-processing intervention. It is advisable to employ advanced geometric correction techniques such as satellite platform models and/or sufficient ground control to ensure that sub-pixel RMS errors are achieved (Johnson & Kasischke, 1998).

Radiometric normalization of the input data is equally critical in radiometric change detection procedures such as CVA, both to minimize detection of spurious changes due to poor normalization, and ensure that changes of small magnitude can be detected and measured. In the long-term studies the images should be chosen based on the monthly, seasonally or annually for change detection processing, to reduce the effects of variability which may not be of interest. The objective of normalization is to correct insofar as possible for differential atmospheric conditions, solar illumination, sensor calibration, phenologic variability, and other influences that produce radiometric 'change' that is not due to fundamental changes in terrain cover or condition. Frequently, the input scene with the highest solar elevation angle and/or widest dynamic range is used as the 'reference' to which other input data are normalized, so as to avoid loss of information due to data compression (Johnson & Kasischke, 1998).

5 APPLICATION

5.1 Study Area and Data Used

Belek is a township with own municipality in Serik district in Turkey's Antalya Province. The Belek region on the Mediterranean coast is located 30 kilometers on the east side of Antalya province (Figure 5.1). It is one of the most prominent centers of Turkey's tourism industry that was discovered in 1984. In Belek, a tourism center located in Antalya province's coastal areas and the fastest growing destination of the country, all tourist facilities have been established in forest lands under the status of conservation forest (Kuvan & Akan, 2005).



Figure 5.1 The map of the study area

Belek, with its 16 km long beach is the main area for tourism investment on the Southern coast of Turkey, ever since the region was declared as a tourism area in 1990 (Figure 5.2). The region's forests have started being sacrificed for golf courses that have experienced a boom. Several golf courses are grouped in two pairs separated by a ten minute drive with most of the hotels in between. By the end of 2001, the total forest area allocated for 39 tourism facilities was 8,625,352 m². The total allocated area constitutes 39.02% of the forested land under the forest regime within the jurisdiction of the Belek Tourism Center (Kuvan & Akan, 2005).

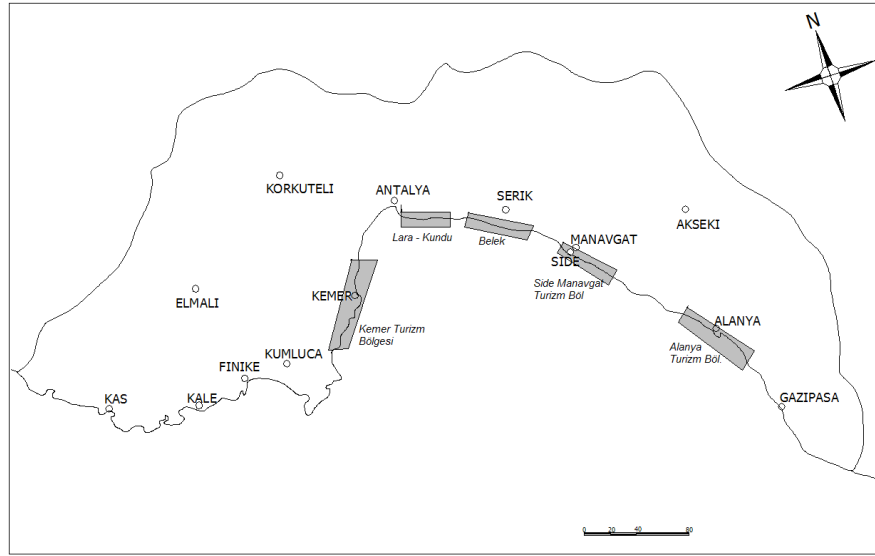


Figure 5.2 Tourism regions of Antalya

The allocation of forest areas to golf fields and touristic facilities kept on over time and can be observed from temporally taken photos from airplanes. The resulting effect of change in land use, from forests to other land covers/uses between 2005 and 2007 can be observed visually from the images given below (Figure 5.3).



Figure 5.3 Aerial photographs of the Belek Forests taken in (a) 2005 and (b) 2007

(© villa-int)

Significant negative impacts and damages to natural and cultural resources have occurred in the coastal zone due to anthropogenic development, mainly as a result of urbanization and tourism (PAP/RAC, 2005).

The SPOT -5 multispectral satellite images of the area covering the forestry and destined areas were acquired and processed by SPOT Image on the 27th of October, 2005 and 23rd of May, 2007 (Table 5.1).

Table 5.1 Spectral and spatial resolutions of the data used

Satellite	Date	Spectral resolution (nm)	Spatial resolution (m)	Processing level
SPOT – 5	27.11.05	Green: 500 – 590	5	Level 2A
	23.05.07	Red: 610 – 680 Near IR: 780 – 890		

5.2 Methodology

Classical digital change detection techniques using multitemporal remotely sensed data taken from the same area are based on the comparison of land cover classifications, multirate classifications, image differencing and ratioing, vegetation index differencing, principal component analysis and change vector analysis. In this study only NDVI differencing and CVA were used as change detection techniques.

The images were processed as Level 2A indicating that a geometric correction was applied to match a standard map projection. The study area was subsetted from the whole scenes and radiometric correction was applied to the after image. The before image was taken as a master while applying min and max normalization. The flow chart followed in this study is given in Figure 5.4. As shown in this figure NDVI was calculated in order to discriminate the vegetated areas from the non-vegetated areas after normalization process. Then the resulted images were subtracted from each other to obtain the difference image. Finally, the CVA technique was performed both to monitor the dynamics and to quantify the vegetation change.

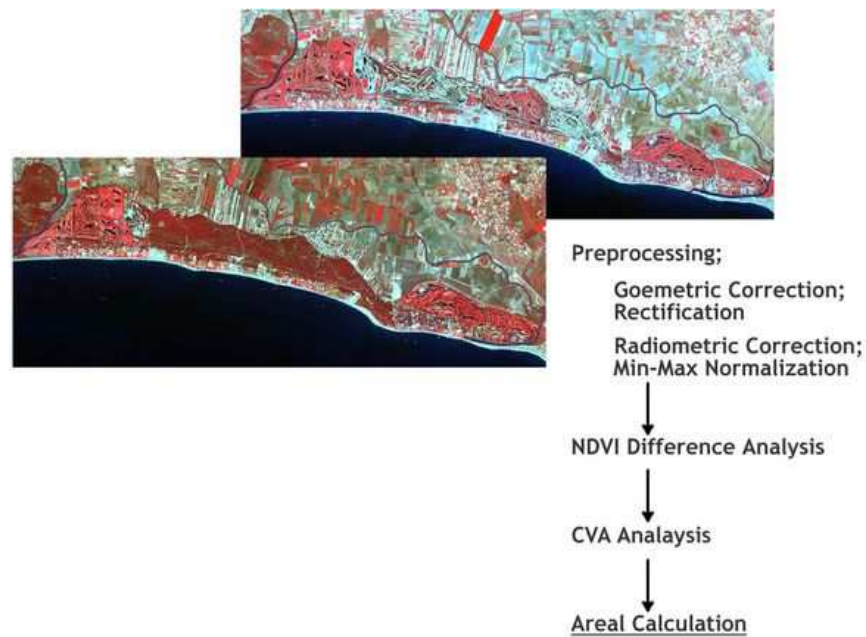


Figure 5.4 Methodology used in this study

5.3 Geometric and radiometric correction

Accurate geometric and radiometric corrections are very important for CVA analysis. In the geometric correction phase, image registration was applied to the after image acquired on 23rd May 07. The GCPs were selected as homogenically as it could be (Figure 5.5). In the registration process, 14 GCP's were used and the RMS error was obtained as ± 0.78 (Figure 5.6).

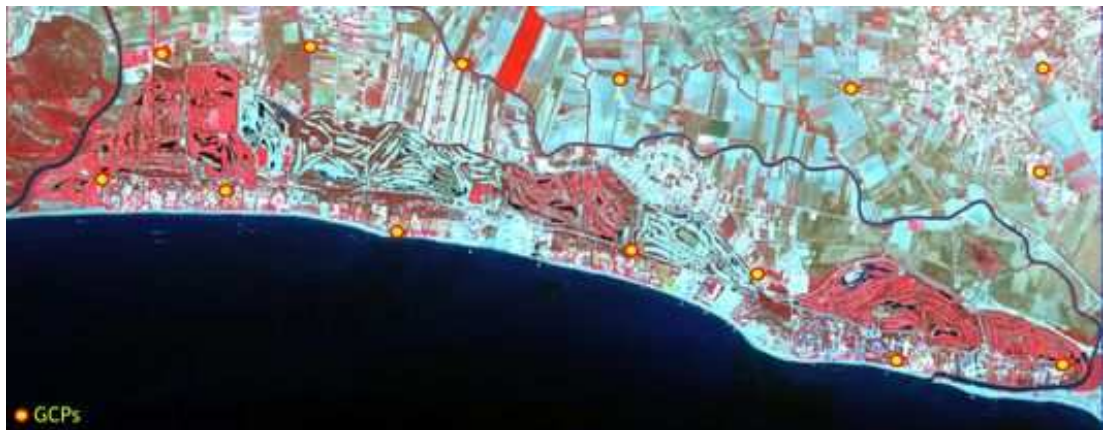
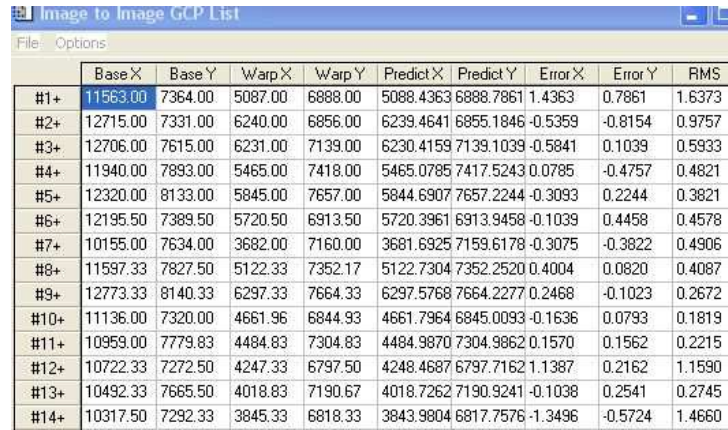


Figure 5.5 The distribution of the GCPs in the second image



	Base X	Base Y	Warp X	Warp Y	Predict X	Predict Y	Error X	Error Y	RMS
#1+	11563.00	7364.00	5087.00	6888.00	5088.4363	6888.7861	1.4363	0.7861	1.6373
#2+	12715.00	7331.00	6240.00	6856.00	6239.4641	6855.1846	-0.5359	-0.8154	0.9757
#3+	12706.00	7615.00	6231.00	7139.00	6230.4159	7139.1039	-0.5841	0.1039	0.5933
#4+	11940.00	7893.00	5465.00	7418.00	5465.0785	7417.5243	0.0785	-0.4757	0.4821
#5+	12320.00	8133.00	5845.00	7657.00	5844.6907	7657.2244	-0.3093	0.2244	0.3821
#6+	12195.50	7389.50	5720.50	6913.50	5720.3961	6913.9458	-0.1039	0.4458	0.4578
#7+	10155.00	7634.00	3682.00	7160.00	3681.6925	7159.6178	-0.3075	-0.3822	0.4906
#8+	11597.33	7827.50	5122.33	7352.17	5122.7304	7352.2520	0.4004	0.0820	0.4087
#9+	12773.33	8140.33	6297.33	7664.33	6297.5768	7664.2277	0.2468	-0.1023	0.2672
#10+	11136.00	7320.00	4661.96	6844.93	4661.7964	6845.0093	-0.1636	0.0793	0.1819
#11+	10959.00	7779.83	4484.83	7304.83	4484.9870	7304.9862	0.1570	0.1562	0.2215
#12+	10722.33	7272.50	4247.33	6797.50	4248.4687	6797.7162	1.1387	0.2162	1.1590
#13+	10492.33	7665.50	4018.83	7190.67	4018.7262	7190.9241	-0.1038	0.2541	0.2745
#14+	10317.50	7292.33	3845.33	6818.33	3843.9804	6817.7576	-1.3496	-0.5724	1.4660

Figure 5.6 The list of the GCPs selected and the errors (X, Y and RMS)

Relative radiometric correction is a method that applies one image as a reference and adjusts the radiometric properties of subject images to match the reference. Relative radiometric correction was preferred depending on the fact that this kind of normalization does not require ancillary datasets on for instance atmospheric conditions and/or aerosol backscatter. Minimum - maximum normalization was chosen and applied to the second image by taking the first image as a master (reference). Each band of the second image was normalized separately using the formula given below.

Normalized DN: $Ax + B$

$$A: (y_{\max} - y_{\min}) / (x_{\max} - x_{\min}) \quad (5.1)$$

$$B: y_{\min} - A x_{\min}$$

In the formulation of minimum - maximum normalization, y_{\max} and y_{\min} represents the max. and min. values of the reference image where x_{\max} and x_{\min} represents the max. and min. values of the image to be normalized. These values were generated from the statistical analyses of the images performed for every band separately (Table 5.2). Then the results were used to generate the equations needed for the min. max. normalization.

$$\begin{aligned} \text{Band 1} & \rightarrow \text{DN: } 0.45 x - 0.7 \\ \text{Band 2} & \rightarrow \text{DN: } 0.52 x - 17.84 \\ \text{Band 3} & \rightarrow \text{DN: } 0.69 x - 45.52 \end{aligned} \quad (5.2)$$

Table 5.2 Min. and max. values of the bands used

Image	Bands	Min. value	Max. value
27.11.05	Band 1 (Near Infrared)	26	255
	Band 2 (Red)	67	255
	Band 3 (Green)	108	255
23.05.07	Band 1 (Near Infrared)	11	115
	Band 2 (Red)	17	116
	Band 3 (Green)	29	131

After the geometric and radiometric corrections applied to the images, the study area was subsetting using an adequate masking is generated by digitization (Figure 5.7).



Figure 5.7 Registered and masked images of the study area

5.4 NDVI differencing

NDVI values of both images were calculated. The resulted images were subtracted from each other (Figure 5.8). The darker (lower NDVI values) areas indicates the non-vegetated areas. However, it is observed that not all the woodcut areas have low NDVI values like it supposed to be.



Figure 5.8 NDVI differencing image

Since the old woodcut areas being sprouted up, these areas have higher NDVI values than forested areas due to the different spectral characteristics of grass and pine trees (Table 5.3) (Figure 5.9) .

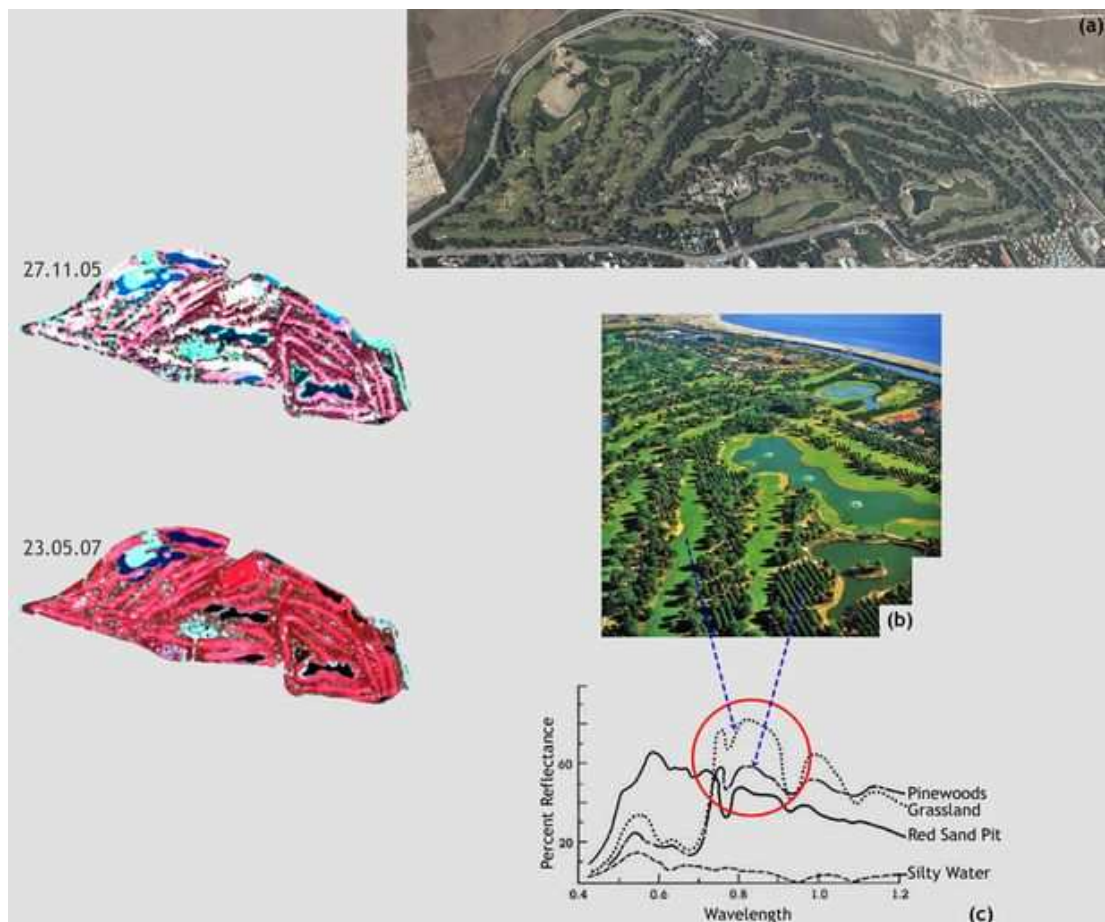


Figure 5.9 An example showing high NDVI difference even though it is a woodcut area. (a) A comparison with the aerial image, (b) Photograph of the area, (c) Spectral reflectance characteristics of grasslands and pinewoods

As a result, areas that were sprouted after woodcutting weren't taken in consideration as deforested areas in the change detection process.

Table 5.3 The appearance of the NDVI difference outputs between the classes in different days

After image	Before image	Appearance of the NDVI difference
Forest	Forest	Grey Tones
Sprout up	Forest	Brighter
Woodcut	Forest	Darker
Sprout Up	Sprout Up	Grey Tones
Sprout Up	Woodcut	Brighter
Woodcut	Woodcut	Grey Tones

5.5 Change vector analysis

The first step of the CVA method was to calculate Soil Brightness Index and Difference Vegetation Index values, in order to reduce the amount of redundant information of the images to be analyzed (Figure 5.10 and Figure 5.11). Spectral change vectors were determined by the change in the variation of the same pixel in multitemporal data within the space formed (Figure 5.12).

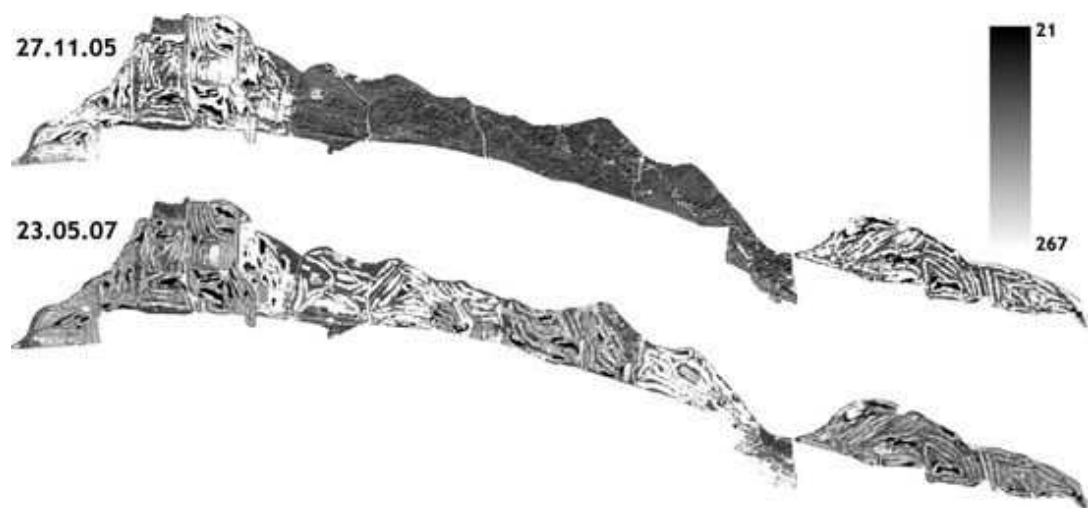


Figure 5.10 Soil Brightness Index images

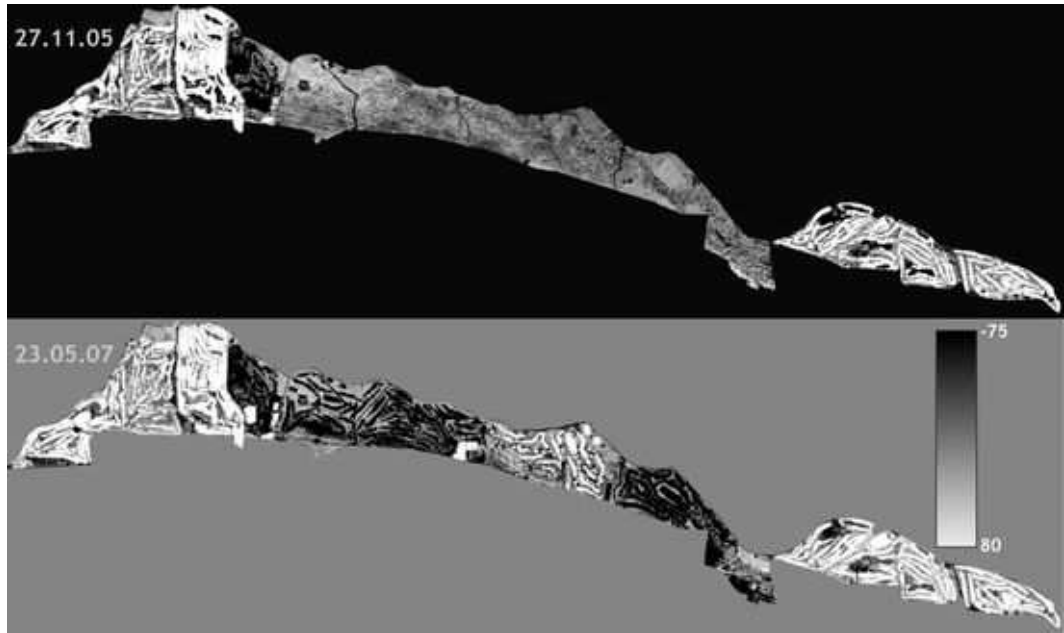


Figure 5.11 Difference Vegetation Index images

The magnitudes of these vectors were then calculated with the Euclidean Distance indicating the differences in positions of the same pixels.

$$R: \sqrt{(y_2 - y_1)^2 + (x_2 - x_1)^2} \quad (5.3)$$

Change direction is measured as the angle of the change vector from a pixel measurement at date 1 to the corresponding pixel measurement at date 2 (Kuzera et al, 2005).

Angles measured between 90° and 180° indicate an increase in DVI and a decrease in SBI that represent regeneration of vegetation. Angles measured between -90° and 0° indicate a decrease in DVI and an increase in SBI that represent deforestation. Angles measured between $0^\circ - 90^\circ$ and $-180^\circ - -90^\circ$ indicate either increases or decreases in both bands of DVI and SBI indicating no change (Kuzera et al, 2005) (Figure 5.12).

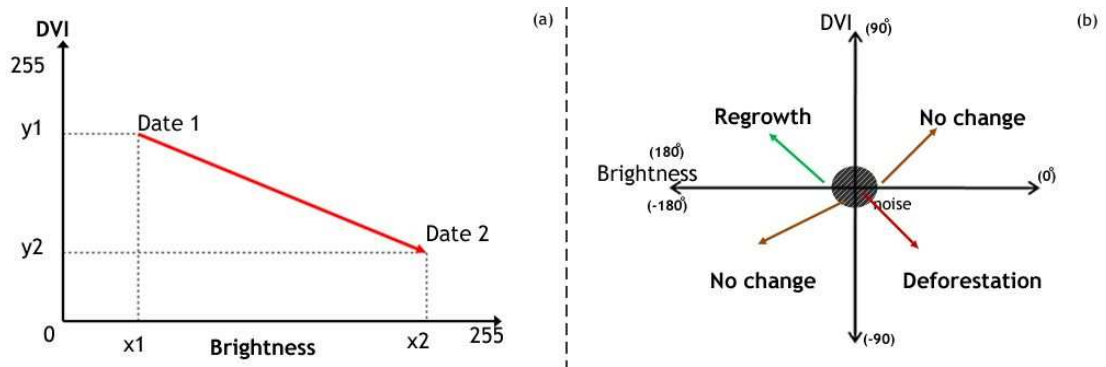


Figure 5.12 The process for detecting (a) the magnitude of change and (b) the direction of change within CVA

The calculation of the direction and the magnitude of change were programmed in Matlab environment (Annex-1). First, the images were transferred to ASCII format by using ENVI software. In order to analyze the images in Matlab environment, the first three lines including the information about the file format, line information and the file location generated by ENVI were deleted (Figure 5.13). Then, the images were loaded in matrix format to Matlab environment. In the code, the masked areas represented with 0.0000 value in the image matrix, weren't included in the calculation process.

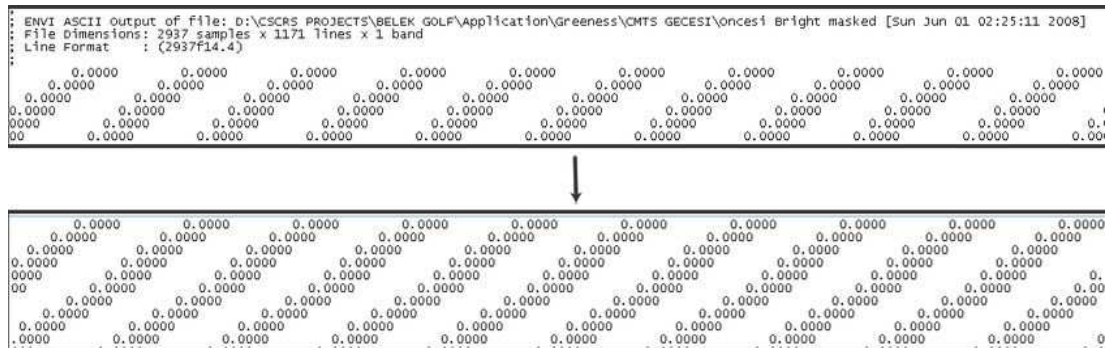


Figure 5.13 Transferring bands to Matlab Environment

First the distance calculation based on Euclidean distance was programmed. When this part is being completed, the min. and max. values of the distance in the images are displayed on the screen for the user. The final phase of the code is the calculation of the magnitude change while defining the change of direction and giving the amount of the total pixels with the percentage.

In order to compute the woodcut areas, another program that uses the results of the CVA analyze was generated (Annex-2). This written code calculates the total area of

the corresponding pixels, which are in the direction of 0° and -90° and greater than a given magnitude. This algorithm enables the user to use the outcome of CVA analyze as an input for the calculation, while the magnitude threshold can be changed without recalculation of the whole components of the CVA. The results were printed as total pixel and/or percentage format.

In order to define the threshold values, the diagram of magnitude distribution was drawn in Matlab environment (Annex 3) (Figure 5.14). The axis of the graph indicates a magnitude value and the total number of pixels that were over the given magnitude value. Depending on the distribution of pixels, the regions where the slopes are changing values from negative to positive (or visa versa) were selected as two threshold values. These values were representing the magnitude value of noise and/or normalization errors and the general deforestation that occur in the study area respectively.

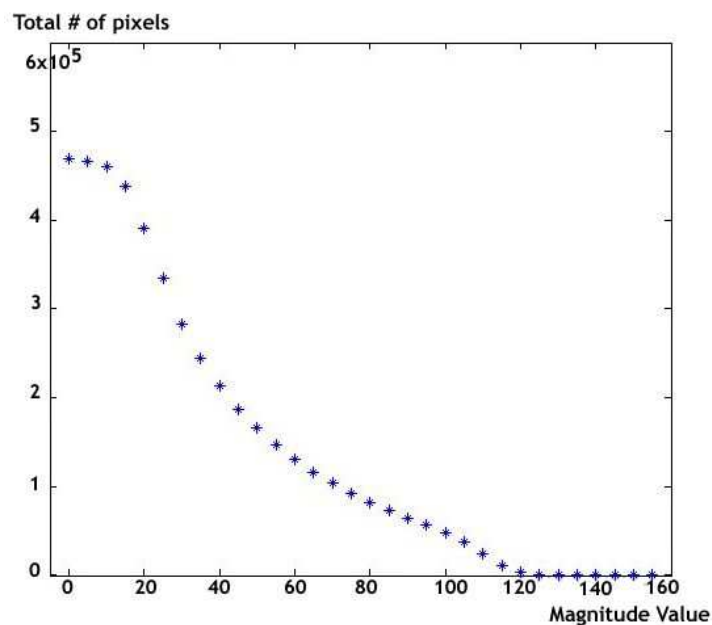


Figure 5.14 The graph indicating the total number of pixel distribution versus magnitude value

A fourth code was written in order to print the results in image format (.tiff) for the visualization (Annex-4). In this code, “before image” was chosen for the base image and the pixels having the adequate specifications were labeled with red color referring to deforestation. In order to be able to use this code, the variables of distance and direction shouldn’t be cleared from the memory of Matlab.

As a threshold value of 26 DN was chosen and the values less than 26 DN were considered as noise or non-efficient normalization (Figure 5.15). Deforested areas that had decrease in DVI and an increase in SBI as the direction of change (i.e. general deforestation) were calculated as 745.8ha.

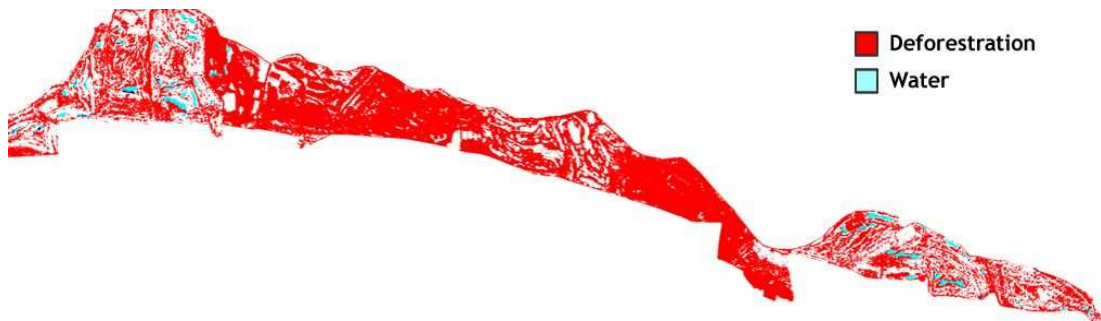


Figure 5.15 Change image – Deforestation in the study area with the threshold value of 26 DN

In order to analyze the deforestation amount for denser forest areas, the threshold value was taken as 80 DN (Figure 5.16). The calculated area indicating the denser deforestation was found as 235.6ha.



Figure 5.16 Change image – Deforestation in the study area with the threshold value of 80 DN

6 RESULTS

Turkey's total forest coverage is 27 percentage of the total land area. This value of forest coverage can be considered sufficient depending on the world forest distribution; however 49 percent of Turkey's forests are non-productive that can be classified as insufficient. Depending on these environmental aspects, the forest areas should be under protection while redoubling the total forest coverage area by planting new trees and preserving. These precautions won't be enough by just themselves. Monitoring the forestlands for any possible change while being able to detect the changes if any, should be the main consideration for sustainable forest management. In this content, remote sensing techniques are very adequate to monitor and detect the changes in land cover/use with high accuracy. The increasing capabilities of satellite platforms and sensors including the newly developed techniques enable the analyzers to gain more power on the researches and obtain better results than before.

There are many techniques developed mainly for change detection and monitoring. These methods were based on the spectral categorization that is called classification and spectral discrimination of change. Both of the methods give satisfactory results for the change detection analyzes. CVA, a relatively new technique, based on the spectral characteristics of the mutitemporal images is being accepted to give reasonable results for the detection of land cover/use change. This method provides information about the magnitude and the direction of change by examining the corresponding pixels of multitemporal images.

In this study, spectral discrimination methods such as band differencing and CVA were used to detect the amount of the change that occurred due to woodcutting in the Belek forestland where it was under government protection until 1984. After 1984, the area began to be a tourism attraction and new spa and golf concept facilities were constructed in order to increase the interest to the area. As a result, the Belek forestland turned out to be golf areas for luxury accommodation facilities in a few years.

In order to analyze the biomass in the area, NDVI was used as an indicator and NDVI differencing was used to gain information about the general change and its detectability. Due to the differences in the spectral characteristics of forestlands and grasslands, NDVI differencing was initiator of for CVA and the regions that can be analyzed as deforestation.

The code of the CVA technique was written in Matlab environment after the calculation of the SBI and DVI components. These indexes were chosen in order to reduce the dimensionality of the band and also highlight the vegetative properties of the landscape. The result of the CVA gave the magnitude of change while indicating its direction. A magnitude threshold value that can be set by the analyzer regarding to the noise or non-efficient normalization, can be used as an input to define different changes of magnitude. The visualization of the obtained results were achieved by another written code based on labelling the pixels having the change with specific (i.e., red) colour referring to deforestation.

It is observed that CVA may reveal an increase in SBI and decrease in DVI, but this alone indicates neither that the changed area was previously forest nor it has changed to non-forest. The areal extent of general deforestation that was indicated with the selected threshold value of 26 is found as 745.8 ha. On the other hand the deforestation of dense forest areas that were indicated with the selected threshold value of 80 is calculated as 235.6 ha between 27th October 2005 and 23th May 2007. In addition to allowing an unambiguous detection of abrupt changes in the forest types, it is thought that CVA approach of multitemporal data is more sensitive to, and provide more information on, subtle changes seasonally, vegetation phenology and ecosystem dynamics than the more classic approaches for which only a few isolated dates from different years or seasons compared.

REFERENCES

- Agouris, P.**, 2005, "Energy Interactions, University of Maine, National Center for Geographic Information & Analysis, Dept. of Spatial Information Science&Engineering", http://www.spatial.maine.edu/~peggy/Teaching/Ch1_B.ppt (Last accessed at 30 April 2007)
- Allen, T. R., Kupfer, J.A.**, 2000, "Application of Spherical Statistics to Change Vector Analysis of Landsat Data: Southern Appalachian Spruce-Fir Forests", *Remote Sensing of Environment* Vol:74, Pg: 482-493.
- Bruzzone, L., Prieto, D.F.**, 2000, "Automatic analysis of the difference image for unsupervised change detection", *IEEE Transactions on Geoscience and Remote Sensing*, 38(3):1171–1182
- Butler, R.A.**, 2006, "Statistics: Turkey", <http://rainforests.mongabay.com/deforestation/2000/Turkey.htm> (Last accessed at 23 May 2008)
- Calgary**, 2003, "An overview of remote sensing", <http://www.ucalgary.ca/UofC/faculties/SS/GEOG/Virtual/Remote%20Sensing/rswat er.html> (Last accessed at 5 April 2008)
- Canbolat, A.F.**, 2000, Conservation of Belek Sea Turtles '99, Final Report, Belek Tourism Investors Association (BETUYAB), Ankara, 142 p. <http://www.strt.hacettepe.edu.tr/english/publications.htm> (Last accessed at 5 April 2008)
- Chen, J., Gong P., He C., Pu R., Shi P.**, 2003, "Land-Use/Land-Cover Change Detection Using Improved Change-Vector Analysis", *Photogrammetric Engineering & Remote Sensing*, Vol. 69, No. 4, April 2003, Pg. 369–379. 0099-1112/03/6904
- CNES** (Centre National d'Etude Spatiales), 2008, "SPOT 5 Observing Earth", <http://132.149.11.105/gb/index3.htm> (Last accessed at 5 April 2008)

CRISP, 2001, “Principles of Remote Sensing”, www.crisp.nus.edu.sg/~research/ (Last accessed at 5 April 2008)

Cyprus Observer, 2007, “Deforestation revealed in Belek”. <http://www.observercyprus.com/observer/NewsDetails.aspx?id=2450>

Didan, K., 2003, “Modis – Introduction”, <http://tbrs.arizona.edu/project/MODIS/index.php> (Last accessed at 15 April 2008)

Ding, Y., Elvidge, C.D., Lunetta, R. S., 1998, “Survey of multispectral methods for land cover change detection analysis, Remote Sensing Change Detection: Environmental Monitoring Methods and Applications”, Sleeping Bear Press, Inc., New York, N.Y., Pg: 21–39

Ekmen, A.E., Topçu, E., 2007, “The economical reasons behind deforestation”, <http://www.deu.edu.tr/userweb/sedef.akgungor/dosyalar/deforestation%20persentation%20-%20env.%20econ.ppt> (Last accessed at 23 May 2008)

FAO (Food and Agriculture Organization of the United Nations), 2008, “Forestry”, <http://www.fao.org/forestry/home/en/> (Last accessed at 15 April 2008)

Fiset, N., 2008, “The effect of deforestation”, <http://ezinearticles.com/?The-Effect-of-Deforestation&id=510236> (Last accessed at 15 April 2008)

Fung, T., Le-Drew, E., 1988, “The determination of optimal threshold levels for change detection using various accuracy indices”, *Photogrammetric Engineering & Remote Sensing*, 54:1449–1454

GA (Geoscience Australia), 2007, “Satellite Facts - The current status of remote sensing satellites and sensors”, <http://www.ga.gov.au/acres/facts.htm> (Last accessed at 7 April 2008)

Hyperphysics, 2005, Electricity and magnetism, Electromagnetic spectrum <http://hyperphysics.phy-astr.gsu.edu/hbase/ems3.html> (Last accessed at 15 April 2008)

Johnson, R. D., Kasischke, E. S., 1998, Environmental Research Institute of Michigan (ERIM), “Change vector analysis: a technique for the multispectral monitoring of land cover and condition”, *International Journal of Remote Sensing*, Vol. 19, No. 3, Pg: 411-426

Kaiser, P., 2008, “All about Belek”, http://www.belek.cx/html/bel_inbrief.htm (Last accessed at 15 April 2008)

Kuvan, Y., 2005, "The use of forests for the purpose of tourism: the case of Belek Tourism Center in Turkey", *Journal of environmental management*, 2005 May;75(3):263-74

Kuvan, Y., Akan, P., 2005, "Residents' attitudes toward general and forest-related impacts of tourism: the case of Belek, Antalya, *Tourism Management* Volume: 26 Issue: 5 Pg: 691–706

Kuzera, K., Rogan, J., Eastman, J. R., 2005, "Monitoring Vegetation Regeneration and Deforestation Using Change Vector Analysis: Mt. St. Helens Study Area", *ASPRS 2005 Annual Conference*, Baltimore, Maryland

Lambin, E., Strahler, A., 1994, "Change-vector analysis in multitemporal space: a tool to detect and categorize land-cover change processes using high temporal-resolution satellite data" *Remote Sensing of Environment*, Vol. 48, Pg:231-244.

Lau, Shiao, C., Kao-Hsing, 1998, "Combined Use of SPOT and GIS Data to Detect Rice Paddies", *Asian Association of Remote Sensing (AARS), Asian Conference on Remote Sensing Proceedings*, November 16-20, Manila

Lawrence, R. L., Ripple, W. J., 1999, "Calculating Change Curves for Multitemporal Satellite Imagery: Mount St. Helens 1980-1995", *Remote Sensing of Environment* Vol:67, Pg: 309-319.

Lillesand, T.M. and Kiefer, R.W., 1987, "Remote Sensing and Image Interpretation", Second Edition, John Wiley & Sons Inc., USA

Lorena, R. B., Santos, J. R., Shimabukuro, Y. E., Brown, I. F., Kux, H. J. H., 2002, "A change vector analysis technique to monitor land use/land cover change in SW Brazilian Amazon: Acre Site" *Proceeding from Integrated Remote Sensing at the Global, Regional, and Local Scale: ISPRS Commission I Mid-Term Symposium in conjunction with Pecora 15/Land Satellite Information IV Conference*, November 10-15, 2002, Denver, Colorado, USA. 8 p.

Lunetta, R. S., Johnson, D. M., Lyon, J. G., Crotwell, J., 2004, "Impacts of imagery temporal frequency on land-cover change detection monitoring", *Remote Sensing of Environment* Vol: 89 Pg: 444-454.

Maccherone, B., 2007, "Modis design concept", <http://modis.gsfc.nasa.gov/about/design.php> (Last accessed at 7 April 2008)

Malila, W. A., 1980. Change vector analysis: An approach for detecting forest changes with Landsat. *Proceedings, Machine Processing of Remotely Sensed Data Symposium*, Purdue University, West Lafayette, Indiana, (Ann Arbor, ERIM), Pg: 326-335.

Mather, P. M., 1987, “Computer Processing of Remotely-Sensed Images”, John Wiley & Sons Inc, Great Britain

Michalek, J.L., Wagner, T.W., Luczkovich, J.J., Stoffle, R.W., 1993, “Multispectral change vector analysis for monitoring coastal marine environments”, *Photogrammetric Engineering & Remote Sensing*, 59:381–384

Nigros, J.E., 2003, Turkey: “May Our Forests Never Thin Out”, <http://www.islamonline.net/english/Science/2003/05/article15.shtml> (Last accessed at 7 April 2008)

NRRI, 2000, NDVI <http://oden.nrri.umn.edu/lsgis/ndvi.htm> (Last accessed at 7 April 2008)

PAP/RAC (Coastal Area Management in Turkey, Priority Actions Programme Regional Activity Centre), 2005, Split, “Coastal Area management in Turkey”, <http://www.medcoast.org.tr/publications/cam%20in%20turkey.pdf> (Last accessed at 18 April 2008)

Rekacewicz P., UNEP/GRID-Arendal, 2002, “Areas affected by deforestation”, <http://maps.grida.no/go/graphic/areas-affected-by-deforestation> (Last accessed at 15 August 2008)

Schneider, D. J., 2007, Michigan Technological University, “Remote Sensing of the Global Environment” <http://www.geo.mtu.edu/rs/back/spectrum/> (Last accessed at 15 April 2008)

Short, N., M., 2007, “Electromagnetic Spectrum: Spectral Signatures”, http://rst.gsfc.nasa.gov/Intro/Part2_5.html, (Last accessed at 18 April 2008)

Siwe, R. N., Koch B., 2008, “Change vector analysis to categorise land cover change processes using the tasselled cap as biophysical indicator”, *Environmental Monitoring and Assessment*, Springer Netherlands, Volume 145, Numbers 1-3, ISSN: 0167-6369 (Print) 1573-2959 (Online)

Smits, P. C., Annoni A., 2000, “Toward specification driven change detection, *IEEE Transactions on Geoscience and Remote Sensing*”, 38(3):1484–1488

Sohl, T.L., 1999, “Change analysis in the United Arab Emirates: An investigation of techniques”, *Photogrammetric Engineering & Remote Sensing*, 65:475–484

SPOT Image, 2008, “The Spot Family”, <http://www.spotasiasg.com.sg/brochures/SPOT%20Family.pdf> (Last accessed at 18 April 2008)

UNEP (United Nations Environment Programme) , 2008, “One planet many people”, <http://www.na.unep.net/OnePlanetManyPeople/chapters.html> (Last accessed at 20 April 2008)

UNESCO (United Nations Educational Scientific and Cultural Organization), 2008, “Deforestation, Desertification”, http://portal.unesco.org/education/en/ev.php-URL_ID=28906&URL_DO=DO_TOPIC&URL_SECTION=201.html (Last accessed at 20 April 2008)

USG Remote Sensing Lab, 1998, “Digital Image Processing”, <http://www.cla.sc.edu/geog/rslab/Rsc/rsc-frames.html> (Last accessed at 8 April 2008)

UTEP, 2002, Resoulution, <http://www.geo.utep.edu/pub/keller/Resolution/Resolution.html> (Last accessed at 20 April 2008)

Virag, L.A., Colwell, J.E., 1987, “An improved procedure for analysis of change in Thematic Mapper image-pairs”, Proceedings of the Twenty-First International Symposium on Remote Sensing Environment, 26-30 October, Ann Arbor, Michigan, Pg. 1101–1110

Xie, Y., Sha, Z., Yu, M., 2008, “Remote sensing imagery in vegetation mapping: a review”, Journal of Plant Ecology, Volume 1, Number 1, Pg 9–23, doi: 10.1093/jpe/rtm005

ANNEX – 1

```
clear all; close all; clc
```

```
test1 = load('C:\Documents and Settings\Administrator\Desktop\CMTS GECESI\B1n.txt');  
test2 = load('C:\Documents and Settings\Administrator\Desktop\CMTS GECESI\B2n.txt');  
test3 = load('C:\Documents and Settings\Administrator\Desktop\CMTS GECESI\D1n.txt');  
test4 = load('C:\Documents and Settings\Administrator\Desktop\CMTS GECESI\D2n.txt');
```

```
B1 = test1;  
B2 = test2;  
G1 = test3;  
G2 = test4;
```

```
R = zeros(1171,2937);  
A = zeros(1171,2937);
```

```
process = 0;  
Str = [];
```

```
for i = 1:1171  
    for j = 1:2937  
        process = process + 1;  
        percent = round(100 * process / (1171*2937*3));  
        disp(['Loading..... ', num2str(percent), ' %'])  
        % Euclidian distance  
        R(i,j) = sqrt((B2(i,j)-B1(i,j))^2 + (G2(i,j)-G1(i,j))^2);  
        % if R(i,j) > 255  
        % Str = [Str; i,j, B1(i,j), B2(i,j), G1(i,j), G2(i,j), R(i,j)];  
        % end  
        A(i,j) = (180/pi)* atan2((G2(i,j)-G1(i,j)),(B2(i,j)-B1(i,j)));  
    end  
end
```

```
plusplus = 0;  
minusplus = 0;  
plusminus = 0;  
minusminus = 0;
```

```
minR = min(min(R))  
maxR = max(max(R))
```

```

threshold = input('enter the threshold = ');

for i = 1:1171
    for j = 1:2937
        process = process + 1;
        percent = round(100 * process / (1171*2937*3));
        disp(['Loading..... ', num2str(percent), ' %'])
        if R(i,j) > threshold
            if A(i,j) == 0
                plusplus = plusplus + 1;
            elseif A(i,j) == 90
                plusplus = plusplus + 1;
            elseif A(i,j) == 180
                minusplus = minusplus + 1;
            elseif A(i,j) == -90
                plusminus = plusminus + 1;
            end
        end
    end
end

for i = 1:1171
    for j = 1:2937
        process = process + 1;
        percent = round(100 * process / (1171*2937*3));
        disp(['Loading..... ', num2str(percent), ' %'])
        if R(i,j) > threshold
            if A(i,j) > 0 & A(i,j) < 90
                plusplus = plusplus + 1;
            elseif A(i,j) > 90 & A(i,j) < 180
                minusplus = minusplus + 1;
            elseif A(i,j) < 0 & A(i,j) > -90
                plusminus = plusminus + 1;
            elseif A(i,j) < -90 & A(i,j) > -180
                minusminus = minusminus + 1;
            end
        end
    end
end

total = plusplus + minusplus + minusminus + plusminus;
plusplus
percentPP = 100 * plusplus/total
minusplus
percentMP = 100 * minusplus/total
minusminus
percentMM = 100 * minusminus/total
plusminus
percentPM = 100 * plusminus/total

```

ANNEX – 2

```
function threshOrman(R,A,threshold)

process = 1171*2937;
plusplus = 0;
minusplus = 0;
plusminus = 0;
minusminus = 0;

for i = 1:1171
    for j = 1:2937
        process = process + 1;
        percent = round(100 * process / (1171*2937*3));
        disp(['Loading..... ', num2str(percent), ' %'])
        if R(i,j) > threshold
            if A(i,j) == 0
                plusplus = plusplus + 1;
            elseif A(i,j) == 90
                plusplus = plusplus + 1;
            elseif A(i,j) == 180
                minusplus = minusplus + 1;
            elseif A(i,j) == -90
                plusminus = plusminus + 1;
            end
        end
    end
end

for i = 1:1171
    for j = 1:2937
        process = process + 1;
        percent = round(100 * process / (1171*2937*3));
        disp(['Loading..... ', num2str(percent), ' %'])
        if R(i,j) > threshold
            if A(i,j) > 0 & A(i,j) < 90
                plusplus = plusplus + 1;
            elseif A(i,j) > 90 & A(i,j) < 180
                minusplus = minusplus + 1;
            elseif A(i,j) < 0 & A(i,j) > -90
                plusminus = plusminus + 1;
            elseif A(i,j) < -90 & A(i,j) > -180
                minusminus = minusminus + 1;
            end
        end
    end
end
```

```

        end
    end
end
end

total = plusplus + minusplus + minusminus + plusminus;
% plusplus
percentPP = 100 * plusplus/total;
% minusplus
percentMP = 100 * minusplus/total;
% minusminus
percentMM = 100 * minusminus/total;
% plusminus
percentPM = 100 * plusminus/total;

disp(['threshold value = ', num2str(threshold)])
disp(['plusplus = ', num2str(plusplus) , ' ', num2str(percentPP), ' %'])
disp(['minusplus = ', num2str(minusplus) , ' ', num2str(percentMP), ' %'])
disp(['minusminus = ', num2str(minusminus) , ' ', num2str(percentMM), ' %'])

disp(['plusminus = ', num2str(plusminus) , ' ', num2str(percentPM), ' %'])

```

ANNEX-3

```
eksen1 = [0:5:155];
eksen2 = [];

for i = 1 : length(eksen1)
    temp = 0;
    for j = 1 : (1171*2937)
        if R(j) > eksen1(i)
            temp = temp + 1;
        end
    end
    eksen2 = [eksen2 temp];
end

% plot(eksen1,eksen2)
% axis([-5 285 -5 3440000])
figure
plot(eksen1,eksen2, '*')
axis([-5 160 -5 600000])
```

ANNEX-4

```
% resmi oku
I = imread('C:\Documents and Settings\Administrator\Desktop\CMTS GECESI\TIF\Oncesi
masked.tif');
IRed = double(I(:, :, 1));
IGreen = double(I(:, :, 2));
IBlue = double(I(:, :, 3));

process = 0;

for i = 1:1171
    for j = 1:2937
        process = process + 1;
        percent = round(100 * process / (1171*2937));
        disp(['Loading..... ', num2str(percent), ' %'])
        if R(i,j) > 35
            if A(i,j) < 0 & A(i,j) >= -90
                IRed(i,j)= 255;
                IGreen(i,j)= 0;
                IBlue(i,j)= 0;
            end
        end
    end
end
end

[a1,a2,a3] = size(I);
I2 = zeros(a1,a2,a3);

I2(:, :, 1)= uint8(IRed);
I2(:, :, 2)= uint8(IGreen);
I2(:, :, 3)= uint8(IBlue);

imwrite(I2,'C:\Documents and Settings\Administrator\Desktop\CMTS
GECESI\TIF\deneme2-2.tif');
```

CV

She was born in Istanbul on 30th September 1982. She graduated from Ata Koleji primary school and Terakki Vakfı Özel Şişli Terakki High School respectively.

She began her higher education in fall 2000 at Istanbul Technical University, Construction Faculty, Geodesy and Photogrammetry Engineering. She got her engineering bachelor degree in 2004 as the third of the semester.

She began her master degree education at Istanbul Technical University, both in Informatics Institute, Satellite Communication and Remote Sensing master programme and Institute of Science and Technology, Geomatic Engineering master programme in 2004. She got her master degree in Geomatic Engineering in 2007.

She is working as a specialist at ITU-CSCRS since 2006 after working as a student assistant for 3 years.